View metadata, citation and similar papers at core.ac.uk

brought to you by CORE

provided by IntechOpen

We are IntechOpen, the world's leading publisher of Open Access books Built by scientists, for scientists

4,800
Open access books available

122,000
International authors and editors

135M
Downloads

Our authors are among the

154
Countries delivered to

TOP 1%
most cited scientists

12.2%
Contributors from top 500 universities

CLARIVATE ANALYTICS BOOK CITATION INDEX INDEXED

WEB OF SCIENCE™

Selection of our books indexed in the Book Citation Index in Web of Science™ Core Collection (BKCI)

Interested in publishing with us?
Contact book.department@intechopen.com

Numbers displayed above are based on latest data collected.
For more information visit www.intechopen.com

8

Magnetic Mn_xGe_{1-x} Dots for Spintronics Applications

Faxian Xiu[1*], Yong Wang[2,3], Jin Zou[2] and Kang L. Wang[4]
[1]*Electrical and Computer Engineering, Iowa State University, Ames, IA*
[2]*Division of Materials, The University of Queensland, Brisbane*
[3]*Materials Science and Engineering, Zhejiang University, Hangzhou*
[4]*Device Research Laboratory, Department of Electrical Engineering*
University of California, Los Angeles, California
[1,4]*USA*
[2]*Australia*
[3]*China*

1. Introduction

Dilute magnetic semiconductors (DMSs) attract tremendous interest as emerging candidates for the microelectronics industry due to their uniqueness in exhibiting spin dependent magneto-electro-optical properties. Their distinctive material characteristics such as spin dependent coupling between semiconductor bands and the localized states promises magnetoelectric effect - the modulation of magnetic properties by an applied electric field - in semiconductors (Kulkarni et al., 2005, Ohno et al., 2000). Thus, a wide variety of semiconductor devices can be envisaged (Brunner, 2002a), such as spin polarized light-emitting diodes, lasers (Schulthess and Butler, 2001, Schilfgaarde and Mryasov, 2001) and spin transistor logic devices (Chen et al., 2005, Brunner, 2002b, Ohno et al., 2000). The development of these devices is considered as a possible route for extending the semiconductor scaling roadmap to spin-added electronics (Liu et al., 2005).

DMS materials can be developed by alloying semiconductors with several percentages of magnetic transition elements (with 3-*d* orbitals), such as Fe, Mn, Co, Ni, and V (Bolduc et al., 2005). The anticipated outcome due to this doping is the fact that the transition elements occupying substitutional sites hybridize with the semiconductor host via the *sp-d* exchange interaction and help to enhance the spin dependent transport, which in turn increase both the magnetization and the Curie temperature (T_c) of the semiconductor system (Jungwirth et al., 2006). This means that the transition metal doping can generate strong spin dependent coupling states in semiconductor systems, which may be further modulated by an electric field (Ohno et al., 2000). Since the band gap engineering and crystal structures of a DMS material are compatible with other semiconductors, they offer significant integration advantages as well (Brunner, 2002a).

* Corresponding Author

The dependence of the transition temperature on the density of mobile carriers is considered as a good evidence for a genuine DMS. However, the key challenge for the growth of DMS materials is the ability to control synthesis of transition metals in semiconductors, aimed at increasing the doping concentration in order to realize room-temperature ferromagnetism. Thus, achieving both semiconducting and ferromagnetic property at room temperature has become a great challenge. Unfortunately, this is hampered by low solubility of transition metal species with a strong tendency to form metallic clusters or heterogeneous regions within the matrix. So the primary research on DMS growth is to produce samples with uniform doping and being free of metallic precipitates.

Substantial theoretical and experimental work were carried out in the past two decades, either to predict or to measure the magnetic properties on a variety of semiconductor materials, including binary and ternary compounds such as III-V, II-VI, IV-VI, VI oxides, III nitrides and group IV systems. Among them, (Ga,Mn)As became the first and the mostly studied DMSs since 1996 (Lu and Lieber, 2006); but to our knowledge, some studies lacked the threshold doping profile to push its curie temperature to room temperature and above (currently around 190 K (Lyu and Moon, 2003, van der Meulen et al., 2008, Maekawa, 2006, Wang et al., 1995)). Since then, substantial research has been carried out in III-V and II-VI semiconductors to improve the T_c by increasing the solubility limit and meanwhile minimizing self-compensation effect of magnetic structures, using radical techniques such as delta doping of modulation doped quantum structures (Bhatt et al., 2002, Cho et al., 2008, Berciu and Bhatt, 2001, Lauhon et al., 2002). Another approach to achieve high-T_c DMS is to use transition metal doped wide bandgap nitrides and oxides, such as GaN, AlN, ZnO, TiO_2. In these materials, high magnetic impurity concentrations are needed due to the lack of long-range interaction among magnetic spins. However, there have been only limited reports on the carrier mediated effect in the wide band gap materials at room temperature (Nepal et al., 2009, Kanki et al., 2006, Philip et al., 2006). Though considerable amount of work has been done on III-V and II-VI DMSs (Ohno et al., 2000, Chiba et al., 2006a), the lack of high T_c and the difficulty in achieving electric field modulated ferromagnetism (carrier mediated ferromagnetism) at or above room temperature deters them from being considered for semiconductor integration.

Group IV semiconductors are of particular interest to the spintronics technology because of their enhanced spin lifetime and coherent length due to their low spin-orbit coupling and lattice inversion symmetry (Rheem et al., 2007, Choi et al., 2005a). There is also considerable interest for transition metal doped group IV semiconductors (Miyoshi et al., 1999, Park et al., 2002, Tsui et al., 2003, D'Orazio et al., 2004, Kazakova et al., 2005, Li et al., 2005, Demidov et al., 2006, Jamet et al., 2006, Collins et al., 2008, Ogawa et al., 2009, Tsuchida et al., 2009) to the semiconductor industry, owing in part to their excellent compatibility with silicon process technology. Several transition metals – including the use of single and co-doping of elements such as Mn, Cr, Co, Fe, Co-Mn, and Fe-Mn – have been used as magnetic dopants in both Si and Ge either through blanket implantation or through *in-situ* doping during epitaxial growth process. Both these materials are reported to be ferromagnetic (Cho et al., 2002, Jamet et al., 2006, Pramanik et al., 2003). The reported experimental results also clearly showed the presence of carrier mediated ferromagnetism in DMS Ge (Chen et al., 2007a, Xiu et al., 2010). A recent study predicted that the T_c could be increased by enhancing the substitutional doping of Mn in Ge and Si, via co-doping - by adding conventional electronic

dopants such as As or P during the Mn doping process (Maekawa, 2004). Theories (Lou et al., 2007) and experiments (D'Orazio et al., 2004, Li et al., 2007) further suggest that the ferromagnetic transition temperature is related to the ratio of interstitial to substitutional Mn similar to that in the group III-V system (Jungwirth et al., 2006).

Considering the fact that, nanosystems such as nanowires and quantum dots (QDs) are the versatile building blocks for both fundamental studies in nanoscale and the assembly of present day functional devices, low dimensional Ge DMS systems such as Mn_xGe_{1-x} nanowires (van der Meulen et al., 2008, Kazakova et al., 2005, Majumdar et al., 2009b, Seong et al., 2009) and QDs (Guoqiang et al., 2008) have also been reported to have room temperature ferromagnetism. The above results are supported by modeling results (Wang and Qian, 2006) although carrier mediated exchange has not yet to be experimentally verified in nanowires. Similarly, high Curie temperatures have been observed in other transition metal doped semiconductor nanostructures such as II-VI (including ZnO (Chang et al., 2003, Cui and Gibson, 2005, Baik and Lee, 2005), ZnS (Brieler et al., 2004, Radovanovic et al., 2005), CdS (Radovanovic et al., 2005)) and III-V (including GaN (Radovanovic et al., 2005, Choi et al., 2005b), GaAs (Jeon et al., 2004)), but only inconclusive reports have been published on the magneto-electric transport in these nanostructures. It could be attributed to the complicated ferromagnetic properties caused by precipitates, second-phase alloys and nanometer-scale clusters. Therefore, it is important and indispensable to differentiate their contributions. Unfortunately, there is still a lack of fundamental understanding of the growth process and spin dependent states in these systems that gives an impetus to extensive investigations into these and related material systems.

In this chapter, we will first introduce the state-of-art theoretical understanding of ferromagnetism in group IV DMSs, particularlly pointing out the possible physics models underlying the complicated ferromagnetic behavior of Mn_xGe_{1-x}. Then, we primarily focus on the magnetic characterizations of epitaxially grown Mn_xGe_{1-x} QDs. It is found that when the material dimension decreases (to zero), it evidences a change of material structures being free of precipitates and a significant increase of T_c over 400 K. The premilinary explanation on these behaviors can be attributed to the carrier confinement in the DMS nanostructures which strengthens hole localization and subsequently enhances the thermal stability of magnetic polarons, thus giving rise to a higher T_c than those of bulk films.

Another important aspect of DMS research lies in the electric field controlled ferromagnetism. We emphasize the existing experimental efforts and achievement in this direction, and provide a detailed description on the field controlled ferromagnetism of the Mn_xGe_{1-x} nanostructuers. We show that the ferromagnetism for the Mn_xGe_{1-x} nanostructures, such as QDs, can be manipulated via the control of gate voltage in a gate metal-oxide-semiconductor (MOS) structure (up to 100 K). These experimental data suggest a hole-mediated ferromagnetism as controlled by a gate bias and promise a potiental of using Mn_xGe_{1-x} nanostructures to achieve spintronic devices. Beyond the scope of DMSs, we will present the metallic Mn_xGe_{1-x} with x~20%, in which a constant Curie temperature was observed. The emphasis, however, is the manipulation of these metallic dots into self-assembled periodic arrays for potential device applications. Finally, we render general comments on the development of the Mn_xGe_{1-x} system and possible research schemes to develop spintronics devices based on this material system.

2. Theories of ferromagnetism in group IV DMS

As in other popular dilute magnetic semiconductors such as (Ga, Mn)As, the formation of magnetic order and the origin of ferromagnetism in Mn_xGe_{1-x} can be described (within the parametric limits) either using complementary mean field approximation models such as the Zener-Kinetic exchange (Ji et al., 2004), the Ruderman-Kittel-Kasuya-Yoshida (RKKY) (Zhao et al., 2003) interaction and percolation theory (Yuldashev et al., 2001) or using density functional theory such as *ab initio* full-potential augmented plane wave (FLAPW) (Stroppa et al., 2003) electronic calculations. Interestingly, the Zener-kinetic exchange model proposed in 1950 could be used for interpreting many of the experimental results in transition metal doped semiconductors (Ji et al., 2007, Akai, 1998, Dietl et al., 2001) besides the transition metals themselves. All the above theoretical approaches have tried to address and to a certain extent successfully answered chemical, electronic and magnetic properties of the transition metal doped group IV semiconductors with in the context of (1) the nature of transition metal impurities, (2) the origin of ferromagnetism, (3) the influence of dopants on the T_c, (4) the solubility limits of carrier density on the chemical nature, (5) the influence of carrier density on the electronic structure, and (6) the influence of different hosts on the electronic structure. Within the above theoretical approaches, these models assume that the ferromagnetism in transition metal doped Ge system is mediated through exchange coupling between the carriers and the interacting lattice. This means that, the interaction is through *p-d* orbital hybridization between the *d* levels and the valence band *p* states of Ge. According to these models, as the number of dopant carriers increases both the electronic mobility and the ferromagnetic ordering of the system also increases along with the T_c. Thus, the assumption is that the strong exchange coupling between the *p* and *d* orbitals leads to strong kinetic exchange coupling between the spin polarized holes and spin polarized TM substitutional vacancies. Among all the 3-*d* TM impurities, [TM=V, Cr, Mn, Fe, Co, Ni], Mn is the most favored dopant. This is because compared to other dopants, Mn favors less clustering, low non-uniform doping distribution and higher substitutional doping over interstitials. The *Ab initio* electronic structure calculations within density functional theory show that, such doping behaviors could result in relatively higher carrier hole concentrations and increased magnetic moments (Park et al., 2002, Stroppa et al., 2003). Complementary theoretical work using the frozen-magnon scheme also shows that the ferromagnetism is produced only through holes and Mn is a good source for generating holes in Ge system (Picozzi and Lezaic, 2008).

In addition, some of the other factors that determine the ferromagnetic strengths in Ge are (1) disorder of Mn site locations, (2) distance between Mn-Mn atoms, (3) solid solubility limits and preferential surface orientation for interstitial and substitution site formation (Luo et al., 2004, Erwin and Petukhov, 2002, Prinz, 1998), and (4) co-doping of Co or Cr with Mn (They were found to reduce cluster formation but not to significantly contribute to the ferromagnetism in the system (Jedema et al., 2002, Chen et al., 2009)). According to full potential linearized augmented plane wave (FLAPW) calculations made on the RKKY model, the coupling between the Mn atoms could be ferromagnetic (FM) or anti-ferromagnetic (AFM) in nature but the interaction is very localized to Mn sites and depends on the distance between Mn atoms: the density of states decreases rapidly as the Ge atom moves away from Mn (Stroppa et al., 2003). However, disorder of Mn site locations is found to influence the ferromagnetic strength and the transition temperature. In addition, the

impact of inherent disorder is also confirmed both by experiments and by the mean field approximation (Valenzuela and Tinkham, 2004, Garzon et al., 2005, Yuldashev et al., 2001). Some of the above models found themselves hard to explain the long range exchange interaction and coupling strength when there is varying dopant concentration and disorder ranging from high resistive state to half metallic state. On the other hand, there are attempts to find solutions for disorder dependent magnetic variation using Percolation theory based mean field approximation calculation (Yuldashev et al., 2001, Schlovskii and L., 1984). Percolation theory provides possible explanations for the experimentally observed low values of saturation magnetization in low carrier density Mn_xGe_{1-x} because the infinite cluster of percolating bound magnetic polarons triggering the long-range ferromagnetic order leaves out a large number of Mn moments at temperatures less than T_c. However, the role of disorder with respect to insulating and conductive metallic phases and their effects on mobility is still not well understood. Conversely, the FLAPW calculations using the density functional theory shows that Mn favors long-range ferromagnetic alignment over short-range anti-ferromagnetic alignment and this increases with the increase of Mn content which is in agreement with many of the experimental results (Stroppa et al., 2003). The estimated Curie temperature is within the range of 134-400 K and is in agreement with experimental and theoretical results (Wang and Qian, 2006).

However, there are also conflicting reports that long range FM order could only happen at low temperature (12 K) and that at low temperature MnGe could show only spin glass behavior due to the inter-cluster formation between the FM Mn-rich clusters (Poli et al., 2006, Lou et al., 2007). With these reports, it is understood that the magnetic phases are more favored over paramagnetic phases by an energy difference of 200 meV/Mn atom (Stroppa et al., 2003). The report also states that the Mn_xGe_{1-x} system is very close to half metallicity irrespective of the amount of doping concentration (Stroppa et al., 2003, Peressi et al., 2005). Electronic band structure calculations using density of states (DOS) show that the binding energy of the Ge 4*s* states are basically unaffected by the exchange splitting of Mn *d* states and the valence band maximum of the minority spin channel in Mn_xGe_{1-x} reaches E_F at Gamma (T) such that the spin gap becomes zero (Stroppa et al., 2003, Peressi et al., 2005). In other words, the DOS shows a valley around E_F and is strictly zero at E_F in the minority spin channel. On the other hand, the energy gap is indirect and the bands around E_F in the majority spin channel arise from Mn *d* and Ge *p* hybridizations so as to give rise to hole pockets closer to the gamma point with a localized magnetic moment of about $3\mu_B$. This could also be explained using chemical and structural configurations of Mn in Ge. The different chemical species determine the relative positions of the anion and cation atomic energy levels in the Mn_xGe_{1-x} while the different anion size dictates essentially the equilibrium lattice constants (Stroppa et al., 2003). This essentially explains the carrier mediated effect in Mn_xGe_{1-x} even though the system is closer to half metallic.

The aim of all these theoretical work is to build foundation for achieving carrier mediated ferromagnetism at temperatures above room temperature. It is understood that this can be achieved only by growing cluster free and uniformly doped Mn_xGe_{1-x} samples. Experimental reports show that T_c as high as 400 K is obtained for cluster free Mn_xGe_{1-x} samples grown (1) using sub-surfactant epitaxial method (Kimura and Otani, 2008) (2) epitaxial QDs (Xiu et al., 2010) and (3) nanowire structures (Kazakova et al., 2005, Majumdar et al., 2009b, van der Meulen et al., 2008). However, there are only very few theoretical

studies depicting the relation between the quantum confinement and its influence on the origin of ferromagnetism in low dimensional DMS structures (Johnson and Silsbee, 1985, Patibandla et al., 2006),(Kelly et al., 2003). It apparently lacks of systematic theoretical study particularly on Mn_xGe_{1-x} QDs. Therefore, it will be interesting to understand the ability of the quantum confinement phenomenon to retain spin polarization in Mn_xGe_{1-x} QDs structure. Studies on III-V QDs using LSDA approximation show that, unlike in the bulk structures, adding a single or multiple carriers in a magnetic QD can both strongly change the total carrier spin and the temperature of the onset of magnetization and this can be modulated by modifying the quantum confinement and the strength of coulomb interactions. These theoretical results must have ramification in the high Curie temperature Mn_xGe_{1-x} QDs as well since our studies also reveal similar characteristics. But, all of the effect including high T_c that we observe cannot be explained without invoking tiny defects either at the interface or on the surface although the conventional transmission electron microscopy (TEM) cannot reveal their existence due to the limited resolution. All of the above material and electronic properties has been studied in order to understand how feasible a DMS material is for carrier mediated ferromagnetism.

3. Growth and characterizations of group IV DMS and nanostructures

3.1 Overview of the Mn doped Ge

As mentioned above, the Ge-based DMS has attracted extensive attention due to its possibility to be integrated with the mainstream Si microelectronics, in which they may be used to enhance the functionality of Si integrated circuits (Park et al., 2002). In particular, the hole mediated effect discovered in Mn_xGe_{1-x} DMS opens up tremendous possibilities to realize spintronic devices with advantages in reducing power dissipation and increasing new functionalities, leading to perhaps normally off computers. To date, there are many reports on the Mn_xGe_{1-x} growth and characterizations by molecular beam epitaxy (MBE)(Park et al., 2002, Li et al., 2005, Jaeger et al., 2006, Jamet et al., 2006, Tsui et al., 2003, Ahlers et al., 2006a, Ahlers et al., 2006b, Bihler et al., 2006, Bougeard et al., 2006, Devillers et al., 2007, Li et al., 2007, Park et al., 2001, Wang et al., 2008a, Pinto et al., 2005b), ion implantation (Park et al., 2005, Lin et al., 2008, Verna et al., 2006, D'Orazio et al., 2002, Liu et al., 2004, Lifeng et al., 2004, Passacantando et al., 2006, Ottaviano et al., 2007), and bulk crystal growth(Cho et al., 2002, Biegger et al., 2007). We can divide them here, for an easier orientation, into two groups: those that cover fundermantal studies of phase formation, ferromagnetism, and transport properties(Park et al., 2002, Li et al., 2005, Majumdar et al., 2009a, Wang et al., 2008a, Gunnella et al., 2005, Liu et al., 2006, Jaeger et al., 2006, Jamet et al., 2006, Li et al., 2006b, Zhu et al., 2004, Miyoshi et al., 1999, Li et al., 2006a, D'Orazio et al., 2003, Zeng et al., 2006, Cho et al., 2002, Liu and Reinke, 2008, Gambardella et al., 2007, Cho et al., 2006, Morresi et al., 2006, Sugahara et al., 2005, Wang et al., 2008b, Ogawa et al., 2009, Ahlers et al., 2006a, Ahlers et al., 2006b, Bihler et al., 2006, Bougeard et al., 2006, Devillers et al., 2007, D'Orazio et al., 2004, Erwin and Petukhov, 2002, Li et al., 2007, Majumdar et al., 2009b, Park et al., 2001, Passacantando et al., 2007, Seong et al., 2009, Chen et al., 2007b, Biegger et al., 2007, Pinto et al., 2005b, Verna et al., 2007, Pinto et al., 2003, Yu et al., 2006, Yada et al., 2008, Tsuchida et al., 2009, Gambardella et al., 2005), and those that aim to minimize cluster formation and enhance Curie temperatures via co-doping methods(Tsui et al., 2007, Paul and Sanyal, 2009, Gareev et al., 2006, Demidov et al., 2006, Collins et al., 2008, Tsui et al., 2003).

Experimental results show that the Mn doping process in Mn_xGe_{1-x} is complex. Both the T_c and the saturation magnetization depend on the interplay of a variety of factors, which are ultimately determined by growth conditions and post-annealing process (Jamet et al., 2006). The concentration and distribution of Mn dopants, the carrier density, the presence of common defects such as Mn interstitials and Mn clusters significantly influence the magnitude and interactions of the magnetic coupling (Biegger et al., 2007). In early 2002, Park *et al.* (Park et al., 2002) pinoeerly demonstrated ferromagnetic Mn_xGe_{1-x} thin films grown by low-temperature MBE. It was found that the Mn_xGe_{1-x} films were *p*-type semiconductors in character with hole concentration of 10^{19}~10^{20} cm^{-3}, and exhibited pronounced extraordinary Hall effect. The T_c of the Mn_xGe_{1-x} thin films increased linearly with Mn concentration from 25 to 116 K (Mn≤3.5 %). Field controlled ferromagnetism was also observed in a simple gated structure through application of a gate voltage (± 0.5 V), showing a clear hole mediated effect at 50 K. Such a small gate voltage presents an excellent comparability with conventional low voltage circuitry. The origin of ferromagnetic order was understood in the frame of local-spin density approximation (LSDA), where strong hybridization between Mn *d* states of T_2 symmetry with Ge *p* states leads to the configuration $e(\uparrow)^2\, T_2(\uparrow)^2\, T_2(\downarrow)^1$, with a magnetic moment of $3\mu_B$. However, the LSDA calculations gave overestimated T_c which was attributed to the incomplete activation of Mn in experiments and the absence of hole compensation in the simulation (Park et al., 2002).

Since then, various preparation techniques were employed in order to produce Mn-doped Ge DMS, including aforementioned MBE (Li et al., 2005, Jaeger et al., 2006, Jamet et al., 2006, Tsui et al., 2003, Ahlers et al., 2006a, Ahlers et al., 2006b, Bihler et al., 2006, Bougeard et al., 2006, Devillers et al., 2007, Li et al., 2007, Park et al., 2001, Wang et al., 2008a, Pinto et al., 2005b), single-crystal growth(Cho et al., 2002, Biegger et al., 2007), and ion implantation(Park et al., 2005, Lin et al., 2008, Verna et al., 2006, D'Orazio et al., 2002, Liu et al., 2004, Lifeng et al., 2004, Passacantando et al., 2006, Ottaviano et al., 2007), aiming to further increase T_c and to obtain the electric field controllability at room temperature (Biegger et al., 2007). Among these efforts, Cho *et al.* (Cho et al., 2002) reported the synthesis of Mn doped bulk Ge single crystals with 6 % of Mn and a high ferromagnetic order at about 285 K via a vertical gradient solidification method. The origin of the high T_c was found to be complex because of the presence of dilute and dense Mn doped regions. Jaeger *et al.* (Jaeger et al., 2006), however, pointed out that the magnetic properties of these samples were clearly dominated by the presence of the intermetallic compound $Mn_{11}Ge_8$. This was indeed observed by Biegger *et al.* (Biegger et al., 2007), where similar Mn_xGe_{1-x} crystals were produced via Bridgman's crystal growth technique and intermetallic compounds were found in both Mn-rich and Mn-poor regions. These experiments suggest that the bulk Mn_xGe_{1-x} crystals produced at over 1000 ^oC may not be an appropriate method for the Mn_xGe_{1-x} DMS preparation (Biegger et al., 2007).

Apart from the bulk cystal growth, MBE has been widely recognized as a power tool for DMS growth since it can provide non-equilibrium conditions to enhance the incorporation of Mn dopant (Park et al., 2002). Via this technique, Mn doping was found to be extremely sensitive to growth conditions, particularlly to the growth temperature. Excellent work in this aspect can be found in references (Jamet et al., 2006, Ahlers et al., 2006b, Park et al., 2001, Bougeard et al., 2006, Li et al., 2007, Demidov et al., 2006, Pinto et al., 2005b). In general, at low growth temperatures (T_b < 120 ^oC), the diffusion of Mn atoms leads to the formation of

Mn-rich nanostructures, such as nanocolumns (Devillers et al., 2007) and nanodots (Bougeard et al., 2006) with irregular shapes. These nanostructures could contain a high Mn concentration up to 38 % (Jamet et al., 2006) while the surrounding matrix remains a low Mn concentration less than 1 %. A perfect lattice coherence was found in the proximity of the nanostructures, indicative of a strong compression for coherent nanostructure and a large tension for the surrounding matrix (Devillers et al., 2007). These observations are in good agreement with therorectial predictions of a spinodal decomposition (Fukushima et al., 2006), which occurs under a layer-by-layer growth mode with strong pairing attraction between Mn atoms and a tendency of surface diffusion of Mn atoms. These theoretical calculations successfully explained the formation of nanostructures in (Ga, Mn)N and (Zn, Cr)Te) (Fukushima et al., 2006, Devillers et al., 2007), which can be also readily applied to the Mn_xGe_{1-x} system (Devillers et al., 2007). The magnetic properties, however, exhibit various characteristics depending on the nanostructure size and the Mn concentration. In most cases, zero-field cooled (ZFC) and field cooled (FC) magnetizations show superferromagnetic properties with a blocking temperature of ~15 K. It is now clear that such a low blocking temperature is originated from the coherent nanostructures with a diameter below several nanometers. Curie temperatures of these nanostructures were also identified to be below 170 K and varied with different Mn concentration. No Mn_5Ge_3 metallic phases were observed at low temperature regime (T_b < 120 ^{o}C).

Dougeard *et al.* (Bougeard et al., 2006) also found that when the dimension of the nanostructures further reduced, the films showed no overall spontaneous magnetization down to 2 K. TEM results were interpreted in terms of an assembly of superparamagnetic moments developing in the dense distribution of nanometer-siezed clusters. In addition to the single crystalline Mn_xGe_{1-x}, homogeneous ampohous nanoclusters were also observed under certain growth conditions and contributed to ferromagnic order below 100 K (Devillers et al., 2007, Sugahara et al., 2005). To render a general understanding of the Mn_xGe_{1-x} magnetic properties, Jaeger *et al.* (Jaeger et al., 2006) presented a detailed study on $Mn_{0.04}Ge_{0.96}$ and $Mn_{0.20}Ge_{0.80}$ thin films grown at low temperatures and related their magnetic behavior to spin-glass. A frozen magnetic state at low temperatures was observed and attributed to the formation of nanostructures. This is in a good agreement with Devillers *et al.* (Devillers et al., 2007). Therefore, it can be concluded that the Mn_xGe_{1-x} magetic semiconductor is not a conventional ferromagnet since its magnetic properties are significantly complicated by the formation of nanostructures and metallic clusters.

When the growth temperature falls into 120~145 ^{o}C, the Mn_5Ge_3 nanoclusters start to develop and dominate the magnetic property with a Curie temperature of 296 K (Devillers et al., 2007, Jamet et al., 2006). This phase, frequently observed at high temperature growth, is the most stable (Mn, Ge) alloy. The other stable compound $Mn_{11}Ge_8$ was also observed in nanocrysllites surrounded with pure Ge (Park et al., 2001). Although they are ferromagnetic, the metallic character considerably jeopardizes their potential for spintronic applications. Under a narrow growth window around 130 ^{o}C, another phase $MnGe_2$ nanocolumns could be developed with a ~33 % of Mn and a T_c beyond 400 K (Jamet et al., 2006). A remarkable feature of these clusters is the large magneto-resistance due to geometrical effects. Further increasing the growth temperature leads to the dominating magnetic behavior from the Mn_5Ge_3 clusters. As the coherent nanostructures grow larger at high temperature growth, higher blocking temperatures (~30 K) were also obtained (Devillers et al., 2007).

To minimize the phase separation, Mn codoping with Co was attempted to stabilize structures at high Mn doping concentration (Tsui et al., 2003, Tsui et al., 2007, Collins et al., 2008). It showed that codoping with Co can dramatically reduce phase separation and diffusion of Mn within the Ge lattice while it magnetically complements Mn. The measured strain states indicate the critical role played by substitutional Co with its strong tendency to dimerize with interstitial Mn. (Collins et al., 2008) The highest T_c achieved so far is about 270 K (Tsui et al., 2003). Similiarly, Gareev *et al*. (Gareev et al., 2006) reported on the codoping of Fe to achieve a T_c of 209 K. Recent poazrized neutron reflectivity measurements provided evidence to show no segregation and lower clustering tendencies for higher Fe doping (Paul and Sanyal, 2009), which further supported co-doping approach in Mn_xGe_{1-x}.

Ion implantation was also attempted due to its efficiency of Mn incorporation (Passacantando et al., 2006). However, extensive experiments revealed that Mn-rich precipitates were developed and buried in a crystalline Ge matrix (Park et al., 2005, Lin et al., 2008, Verna et al., 2006, D'Orazio et al., 2002, Liu et al., 2004, Lifeng et al., 2004, Passacantando et al., 2006, Ottaviano et al., 2007) in a much similar manner to that of the thin films grown by MBE (Park et al., 2001, Bougeard et al., 2006, Li et al., 2007, Demidov et al., 2006).

Although there has been much progress in producing high quality Mn_xGe_{1-x} thin films, the formation of uncontrollable metallic clusters yet remains a challenge. High T_c DMS thin films without any precipitations seem to be a critical obstacle for the fabrications of practical spintronic devices functioning at room temperature, not to mention the room-temperature controlled ferromagnetism.

3.2 Mn_xGe_{1-x} by molecular beam epitaxy

To gain further insight into the complex growth of this material system, we have performed detailed structural and magnetic characterizations of Mn_xGe_{1-x} grown by MBE with different thickness. Our experiments showed that the Mn doping behavior and magnetic properties are dramatically different when the material dimension becomes smaller. (Chen et al., 2007a, Xiu et al., 2010) Bulk Mn_xGe_{1-x} films always tend to form clusters no matter what growth conditions are. When it comes to one and zero dimensions, however, the cluster formation may be possibly limited because the Mn concentration cannot accumulate enough and the strain can be easily accommodated to minimize the metallic clusters (Wang et al., 2008a, Ottaviano et al., 2007). We further show that self-assembled Mn_xGe_{1-x} DMS QDs can be successfully grown on Si substrate with a high T_c in excess of 400 K. Finally, the electrical field controlled ferromagnetism was also demonstrated in MOS structures using these QDs as the channel layers, as elaborated in section 4.

3.2.1 Self-assembled DMS Mn_xGe_{1-x} QDs

$Mn_{0.05}Ge_{0.95}$ QDs were grown on *p*-type Si substrates. Cross-section TEM was carried out to determine the structural characteristics and the Mn composition. HR-TEM image reveals that a QD has a dome shape with a base diameter of about 30 nm and a height of about 8 nm (Fig. 1(a)) The interface between the dot and the Si substrate has excellent lattice coherence. A careful inspection reveals that the dot is single-crystalline without evidence of pronounced dislocations or stacking faults. However, because of the heavy Mn doping it is

possible that some amount of point defects (such as Mn interstitials) may be present inside the dot, which is beyond the detect capability of conventional TEM.

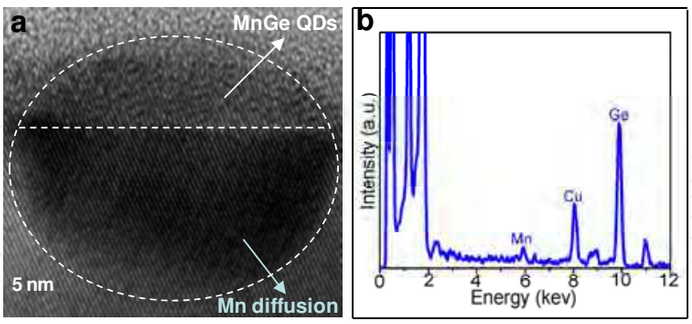

Fig. 1. Structural properties of $Mn_{0.05}Ge_{0.95}$ quantum dots grown on a *p*-type Si substrate. (a) A high-resolution TEM cross-section image of typical $Mn_{0.05}Ge_{0.95}$ quantum dot showing the detailed lattice structure. (b) Typical EDS spectrum showing that both Mn and Ge are present in the $Mn_{0.05}Ge_{0.95}$ quantum dot. The average Mn concentration in the quantum dots was estimated to be 4.8±0.5 %.

Directly underneath the $Mn_{0.05}Ge_{0.95}$ QD, Mn diffuses into Si substrate and forms a strained MnSi area, which has the same diameter as the top $Mn_{0.05}Ge_{0.95}$ QD, but a height of about 16 nm (Fig. 1(a)). This diffusion behavior is not unusual as it was also observed in (In, Mn)As and (In, Cr)As QDs systems. (Holub et al., 2004, Zheng et al., 2007) However, the migrations of Mn into the substrate make it difficult to accurately determine Mn concentration inside the dot. To address this challenge, we have performed energy dispersive x-ray spectroscopy (EDS) experiments (in a scanning TEM mode) to analyze the Mn composition at nanoscale (Fig. 1(b)). When the EDS was performed, electron probes with several nanometers in diameter were illustrated on the $Mn_{0.05}Ge_{0.95}$ QDs and their underlying Si substrate. Consequently Si peaks are constantly observed in the EDS spectra. To estimate the Mn concentrations, we performed a quantitative analysis of atomic percentages of Mn and Ge and artificially discounted the Si peak. The EDS analysis over many QDs reveals a Mn/Ge atomic ratio of about 0.144:1. Since approximately 1/3 volume fraction of Mn is distributed in the Mn_xGe_{1-x} QD (Xiu et al., 2010), the average Mn concentration can be estimated to be 4.8 ± 0.5 %. Note that the deviation was determined by a thorough study of many $Mn_{0.05}Ge_{0.95}$ QDs. Both the HR-TEM investigations and the composition analysis suggest that each individual QD is a single-crystalline DMS system.

Magnetic properties were studied using a superconducting quantum interference device (SQUID) magnetometer at various temperatures. Figure 2(a) and two corresponding insets show the temperature-dependent hysteresis loops when the external magnetic field is parallel to the sample surface (in-plane). The field-dependent magnetization indicates a strong ferromagnetism above 400 K. The saturation magnetic moment per Mn atom is roughly estimated to be 1.8 μ_B at 5 K. A fraction of roughly 60 % of Mn is estimated to be activated assuming that each Mn has a moment of 3 μ_B (Park et al., 2002, Stroppa et al., 2003). The Arrott plots were also made in order to evaluate the T_c (Ohno et al., 2000) (Fig. 2(b)). By neglecting the high order terms, the magnetic field can be expressed in the following equation (Arrott, 1957),

$$H = \frac{1}{\chi}M + \beta M^3 \quad \text{or} \quad \frac{H}{M} = \frac{1}{\chi} + \beta M^2 \tag{1}$$

where H is the external magnetic field, M is the magnetic moment from the sample, χ is the susceptibility, and β is a material dependent constant.

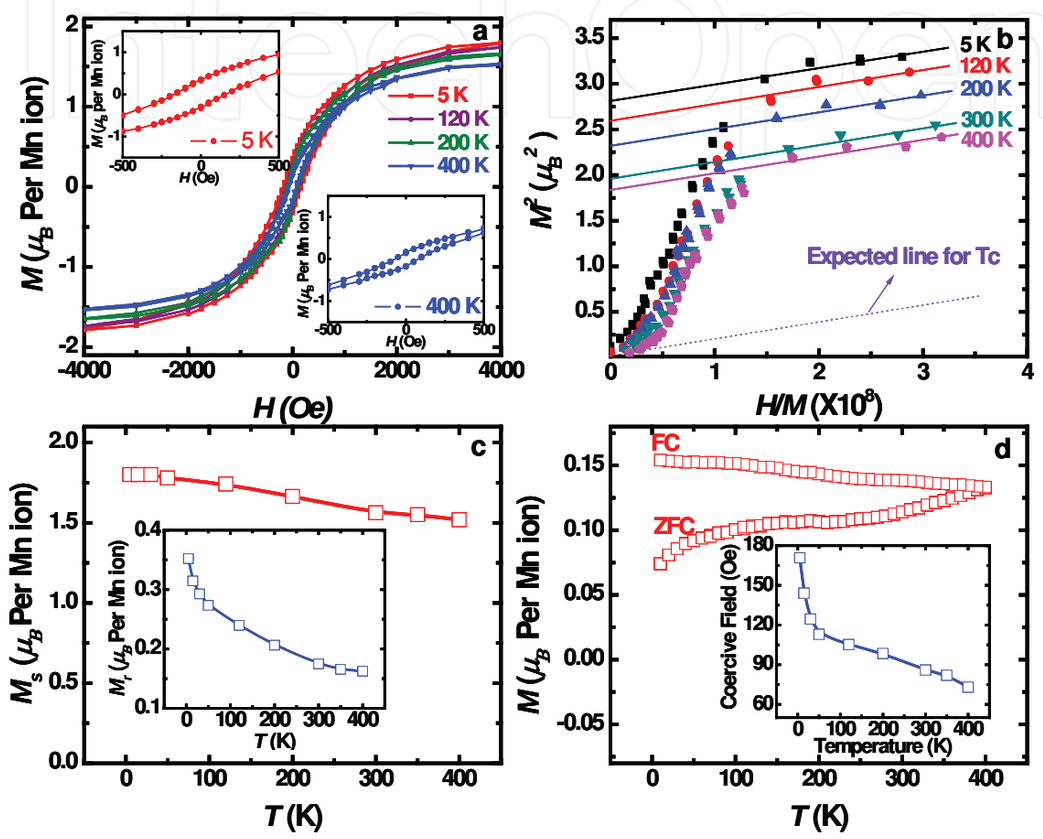

Fig. 2. Magnetic properties of the $Mn_{0.05}Ge_{0.05}$ quantum dots grown on a *p*-type Si substrate. (a) Hysteresis loops measured at different temperatures from 5 to 400 K. (b) The Arrott plots were made to obtain the Curie temperature. Consistent with (a), the Curie temperature is projected to be above 400 K; (c) The temperature dependence of saturation moments. The inset gives the remnant moments with respect to temperature; (d) Zero-field cooled and field cooled magnetizations of quantum dots with a magnetic field of 100 Oe; the inset shows the coercivity values at different temperatures. The external magnetic field is in parallel with the sample surface.

According to Equation (1), M^2 can be plotted as a function of H/M. When H/M is extrapolated to $M^2=0$, the intercept on the H/M axis gives $1/\chi$. The T_c for this material can be obtained when $1/\chi$ vanishes. Figure 2(b) shows the Arrott plots at several temperatures. It can be seen that even at 400 K the intercept ($1/\chi$) on the H/M axis does not vanish, which means that the susceptibility still has a finite value and the T_c has not been reached yet. By using the slope obtained at 400 K, a dashed line can be drawn as shown in Fig. 2(b), in which

a T_c is projected to be beyond 400 K. This is in a good agreement with the data from the hysteresis loops showing the magnetic order above 400 K. Figure 2(c) and corresponding inset show the temperature-dependent saturation and remnant moments per Mn ion, respectively. Both of them demonstrate weak temperature dependences and substantial amount of magnetization moments remain even at 400 K.

ZFC and FC magnetizations were measured with a magnetic field of 100 Oe as shown in Fig. 2(d). The magnetic moments do not drop to zero, suggesting a high T_c beyond 400 K, which is in a good agreement with the Arrott plots in Fig. 2(b). From these two curves, one can also infer the formation of a single phase in this material system, *i.e.*, DMS QDs. The wide separation of the ZFC and FC curves in the temperature range of 5 to 400 K shows the irreversibility of susceptibilities, possibly arising from strain-induced anisotropy as a large lattice mismatch exists between Si and Ge (Dietl et al., 2001). The temperature-dependent coercivity is shown in Fig. 2(d) inset. The coercivity decreases from 170 Oe (at 5 K) to 73 Oe (at 400 K). The small coercivity in the entire temperature range measured features a soft ferromagnetism which originates from Mn ions diluted in the Ge matrix (Kazakova et al., 2005). The above magnetic properties support the fact that the $Mn_{0.05}Ge_{0.95}$ QDs exhibit a DMS type ferromagnetic order.

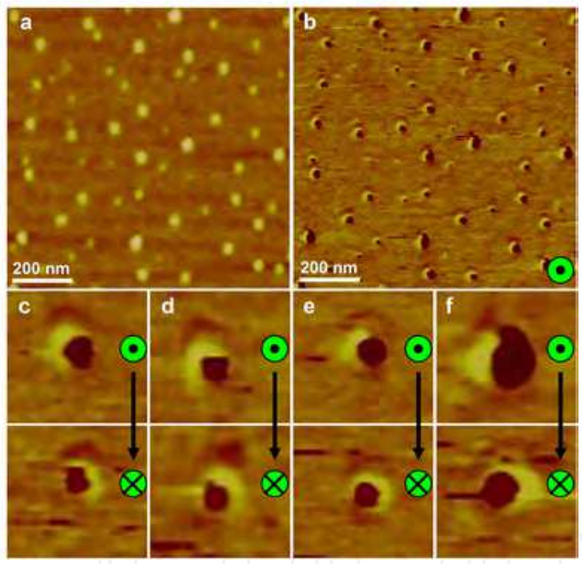

Fig. 3. AFM and MFM images of the $Mn_{0.05}Ge_{0.95}$ quantum dots measured at 320 K. (a) Typical AFM image of $Mn_{0.05}Ge_{0.95}$ quantum dots; (b) Corresponding MFM image with the tip magnetization pointing toward the sample; (c)~(f), Enlarged MFM images of individual quantum dots taken from (b). From these MFM measurements, opposite contrasts were observed when applying an opposite magnetization to the tip.

Atomic force microscopy (AFM) and magnetic force microscopy (MFM) measurements were carried out to investigate the morphology and ferromagnetism of $Mn_{0.05}Ge_{0.95}$ QDs at 320 K, respectively. The average dot size is 50 nm in base diameter and 6 nm in height. The dot density is about 6×10^9 cm^{-2} (Fig. 3(a)). The corresponding MFM image was taken by lifting up the MFM probe 25 nm above the topographic height of the sample in a phase detection mode (Fig. 3(b)). The appearance of bright-and-dark areas in the MFM image clearly shows the

formation of magnetic domains in the $Mn_{0.05}Ge_{0.95}$ QDs, which is similar to (In, Mn)As DMS QDs (Jeon et al., 2002). Figures 3(c)~3(f) show enlarged MFM images of several individual $Mn_{0.05}Ge_{0.95}$ QDs. By reversing the tip magnetization, opposite contrast was observed for each dot, indicating that the magnetic signals originated from the top $Mn_{0.05}Ge_{0.95}$ QDs. Note that each QD is a single domain "particle". During the magnetization process, the domain would rotate preferentially along the magnetic field to produce net magnetization moments. Since the experiments were performed at 320 K, the formation of metallic phases such as Mn_5Ge_3 and $Mn_{11}Ge_8$ can be easily ruled out because they have low Curie temperatures of 296~300 K. Overall, the above MFM results agree well with the TEM observations and the ferromagnetic order at high temperature obtained in the SQUID measurements.

3.3 Discussions

We have reviewed the growth of $Mn_{0.05}Ge_{0.95}$ by MBE, ion implantation, and bulk sintering, emphasizing the growth temperature effect on the phase formation and magnetic properties. While the current motivation is driven by the prospect of enhancing Curie temperatures, the experiments show a strong tendency of metallic precipitates developed in bulk and relatively thick Mn_xGe_{1-x} crystals. The fundermental understanding here points to a spin-glass-like feature in Mn_xGe_{1-x} due to the formation of various lattice coherent nanostructures and metallic precipitates, which exhibit magnetic blocking behaviors under different temperature regimes. The challenge to eliminate these clusters seems to be overwhelming and nearly impossible. However, when the material dimension decreases, it evidences a change of material structures being free of precipitates and a significant increase of Curie temperatures over 400 K. The premilinary explanation on these behaviors can be attributed to the carrier confinement in a DMS QD which strengthens hole localization and subsequently enhances the thermal stability of magnetic polarons giving rise to a higher T_c than those of bulk films. Nevertheless, the experimental data suggest that with nanoscale structures, the quantum confinement effect comes into being which significantly influences the exchange coupling between the confined holes and the localized Mn^{2+}. Future progress in this direction will involve a detailed theoretical treatise to understand the quantum confinement effect on magnetic properties in a quantitive picture.

4. Electric field controlled ferromagnetism

4.1 Introduction

Electric field control of ferromagnetism has a potential to realize spin field-effect transistors (spin FETs) and nonvolatile spin logic devices via carrier-mediated effect (Awschalom et al., 2002, Chiba et al., 2006b). With the manipulation of carrier spins, a new generation of nonvolatile (green) computing systems could be eventually developed for many low-power-dissipation applications in all fields, including sensor network, health monitoring, information, sustainable wireless system, etc. Since Datta and Das (Datta and Das, 1990) first introduced the concept of spin FETs in 1990, enormous efforts were dedicated to creating a device wherein the carrier transport is modulated by electrostatic control of carrier spins (Philip et al., 2006, Ohno et al., 2000, Appelbaum and Monsma, 2007, Chiba et al., 2006a, Nazmul et al., 2004, Nepal et al., 2009, Koo et al., 2009, Chiba et al., 2008, Boukari et al., 2002). To understand and exploit this controllability, several theoretical models were

proposed to explain the ferromagnetic coupling in DMS on a microscopic scale (also elaborated in the theoretical section): the Zener Kinetic-exchange (Jungwirth et al., 2006), double-exchange (Dietl et al., 2000), the RKKY interaction (Matsukura et al., 1998, Yagi et al., 2001). These models share a common feature that a spontaneous ferromagnetic order is carrier-mediated through the increase of carrier concentrations. One of major challenges, however, is to search an ideal material with room-temperature controllable spin states (Philip et al., 2006, Kanki et al., 2006, Dietl and Ohno, 2006). In recent years, emerged DMSs became one of the promising candidates since they could possibly offer high T_c in excess of 300 K (Dietl et al., 2000). The demonstration of the carrier medicated ferromagnetism involving correlated electron/hole systems leads to a para- to ferro-magnetism phase transition (Park et al., 2002, Dietl et al., 2000, Chen et al., 2007a, Chiba et al., 2006b). In principle, the collective alignment of spin states in these DMSs can be manipulated by the modulation of carrier concentrations through gate biasing in a FET structure (Ohno et al., 2000, Dietl and Ohno, 2006). For this kind of spin FETs, the "source" and "drain" may be completed through "nanomagnet", which are in turn controlled by the gate; and no carrier transport is needed. Clearly, one may also involve the control of source-drain conductance by gate-voltage-induced precession of injected spins (from the source). Since early 2000s, a significant progress was achieved (Ohno et al., 2000, Chiba et al., 2006a, Chiba et al., 2008, Chiba et al., 2006b), in which the ferromagnetism of a (In, Mn)As channel layer could be effectively turned on and off via electric fields in a gated FET. Such extraordinary field modulated ferromagnetism immediately rendered the development of future spintronic devices. However, the manipulation of ferromagnetism was limited because of low T_c of the Mn-doped III-V materials (Weisheit et al., 2007). Therefore, a search for new DMS materials with T_c>300 K and carrier mediated ferromagnetism becomes a current global challenge (Jungwirth et al., 2006, Dietl and Ohno, 2006).

4.2 Electric field controlled ferromagnetism in self-assembled DMS $Mn_{0.05}Ge_{0.95}$ QDs

Since the self-assembled $Mn_{0.05}Ge_{0.95}$ QDs have a high T_c above 400 K and are free of metallic phases (Mn_5Ge_3 and $Mn_{11}Ge_8$), it can be potentially used as a channel layer in a MOS device to study the modulation of ferromagnetism by electric field. The device structure consists of a metal gate (Au, 200 nm), Al_2O_3 (40 nm), $Mn_{0.05}Ge_{0.95}$ QDs (6 nm), a wetting layer (<0.6 nm), a *p*-type Si substrate (1×10^{18} cm^{-3}), and a back metal contact (Au, 200 nm). A relative thick dielectric of Al_2O_3 (40 nm) is employed to ensure a small leakage current to a level below 10^{-6} A/cm^2. Figure 4 shows the electric field controlled ferromagnetism performed at 50, 77, and 100 K, corresponding to (a)-(c), (d)-(f), and (g)-(i), respectively. Due to the similarity of the data, we take 77 K as an example to describe the device operation in Figs. 4(d)-4(f). Figures 4(d) and 4e) show the hysteresis loops by SQUID with negative and positive biases on the MOS gate at 77 K, respectively. Under a negative bias, the holes are attracted into the channel of the device (accumulation). In this circumstance, however, the hysteresis loop does not show a remarkable change (Fig. 4(d)). This could be explained by the fact that even at 0 V, the QDs device is already accumulated with enough holes to induce ferromagnetism. In other words, the hole mediated effect is sufficient to align a majority of the activated Mn ions along one direction in each individual QD. Further increasing negative bias does not change much on the hole concentrations. On the contrary, with the positive bias, a large amount of holes are depleted into the *p*-type Si so that hole mediated effect is notably reduced. In fact, the surface of the device can have a high concentration of electrons if the

leakage is limited (Inversion). As a result, the Mn ions start to misalign because of the lack of holes. The saturation moment per Mn ion decreases more than 10 times as the gate bias increases from 0 to + 40 V (Fig. 4(e)). It should be noted that, at +40 V, the saturation and remnant moments of the $Mn_{0.05}Ge_{0.95}$ QDs become fairly weak, resembling a "paramagnetic-like" state. Figure 4(f) summarizes the change of remnant moments as a function of gate voltage. A similar trend in the carrier density as a function of the gate bias was observed from CV curves (not shown here), suggesting a strong correlation between hole concentrations and the ferromagnetism, *i.e.* the hole-mediated effect. The inset in Fig. 4(f) displays an enlarged picture to clearly show the change of remnant moments with respect to the gate bias. By increasing the measurement temperature to 100 K (Figs. 4(g)-4(i)), the modulation of the ferromagnetism becomes less pronounced compared to those at 50 and 77 K due to the increased leakage current in our MOS devices. The above results evidently demonstrate that the hole mediated effect does exist in this material system.

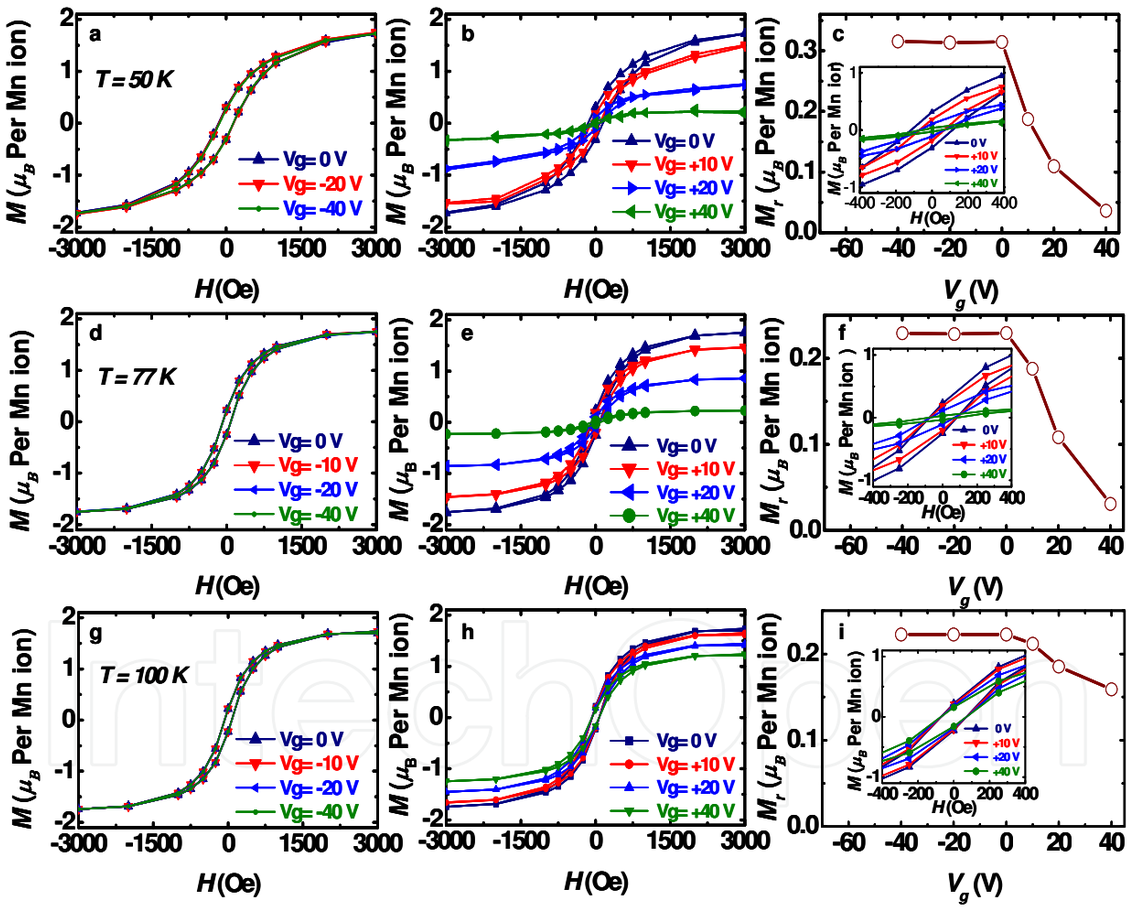

Fig. 4. Control of ferromagnetism of $Mn_{0.05}Ge_{0.95}$ quantum dots by applying electric field at 50 K ((a)~(c)), 77 K ((d)~(f)), and 100 K ((g)~(i)). (a), (d), and (g): Hysteresis loops with zero and negative bias of -10, -20 and -40 V on the gate; (b), (e), and (h): The hysteresis loops with zero and positive bias of +10, +20, and +40 V; (c), (f), and (i): Remnant moments with respect to the gate bias. Insets of (c), (f) and (i) are enlarged figures from the central part of (b), (e) and (h) to clearly show the change of remnant moments, respectively.

4.3 Discussions

Electrical field controlled ferromagnetism has been successfully demonstrated in Mn-doped III-V DMSs (Chiba et al., 2008, Chiba et al., 2006b, Chiba et al., 2006a, Dietl and Ohno, 2006, Ohno et al., 2000). It is well established that the variation of hole concentrations renders such a controllability. (Ohno et al., 2000) The low T_c of III-V DMS, however, presents a challenge to further realize room-temperature controlled ferromagnetism (Weisheit et al., 2007). Alternatively, the recent experiments on $Mn_{0.05}Ge_{0.95}$ QDs show a high T_c above room temperature and gate modulated ferromagnetism over 100 K (Xiu et al., 2010). While the leakage current suppressed the gate modulation, room-temperature controlled ferromagnetism would not be impossible because of the high T_c of this system. Research in this direction may open up a pathway for achieving room-temperature Ge-based (and other) Spin-FETs and spin logic devices. These spintronic devices could potentially replace the conventional FETs with lower power consumptions and provide additional new device functionalities, which is beyond today's mainstream CMOS technology of microelectronics.

5. Metallic Mn_xGe_{1-x} (x~20%) nanodot arrays

5.1 Introduction

There is also a need to develop ferromagnet/semiconductor hybrid structures for semiconductor spintronics since they have magnetic and spin-related functions and excellent compatibility with semiconductor device structures. (Tanaka, 2002, Wang et al., 2011) By embedding magnetic nanocrystals into conventional semiconductors, a unique hybrid system can be developed, allowing not only utilizing the charge properties but also the spin of carriers, which immediately promises next-generation non-volatile magnetic memories and sensors. (Dietl, 2006, Kuroda et al., 2007) On the other hand, spin-injections into the semiconductor can be dramatically enhanced via coherent nanostructures, which considerably reduce undesired spin scatterings. (Kioseoglou et al., 2004) Although magnetic hybrid systems, such as MnAs/GaAs, have been extensively studied over several decades, the control (over the spatial location, shape and geometrical configuration) of the magnetic nanostructures (for instance MnAs) still remains a major challenge to further improve the performance of the related magnetic tunnel junctions (MTJs) and spin valves. (Dietl, 2008)

5.2 Growth methods

We employed a concept of stacked Mn_xGe_{1-x} (x~20%) (Hereafter, we denote it as MnGe) nanodots by alternatively growing MnGe and Ge layers with designated thicknesses (nominal 3 nm thick MnGe and 11 nm thick Ge). It is well known that Mn doping in Ge induces compressive strain because of its larger atomic size, (Slater, 1964) assuming that no lattice defects are generated during the doping process, i.e., lattice coherence. Mn-rich MnGe nanodots induced by the spinodal decomposition should be strained if the lattice coherence between the nanodots and the matrix remains. Once the strained nanodots are developed, a thin Ge spacer layer, subsequently deposited with an optimized thickness, will retain the perfect lattice coherence with the underneath nanodots. This enables the existing nanodots to exert strain on the Ge spacer layer and produce "strained spots", which, in turn, become preferred nucleation sites for successive nanodots. Eventually, multilayered and vertically aligned MnGe nanodot arrays can be produced, similar to the

scenarios of stacked InAs/GaAs (Xie et al., 1995, Solomon et al., 1996) and Ge/Si (Liao et al., 2001) quantum dots. Indeed, by employing this innovative approach, we achieved the growth of coherent self-assembled MnGe nanodot arrays with an estimated density of 10^{11}~10^{12} cm^{-2} within each MnGe layer.

Ten periods of MnGe nanodots were epitaxially grown on Ge (100) and GaAs (100) substrates by the MBE system. TEM and EDS in the scanning TEM (STEM) mode were performed to understand the nanostructures and compositional variations of the resulting thin films. Figure 5a and c are typical plane-view and cross-sectional TEM images and show the general morphology of the MnGe nanostructures, viewed along the <100> and <011> directions, respectively. A high-density of dark nanodots can be clearly seen in both cases.

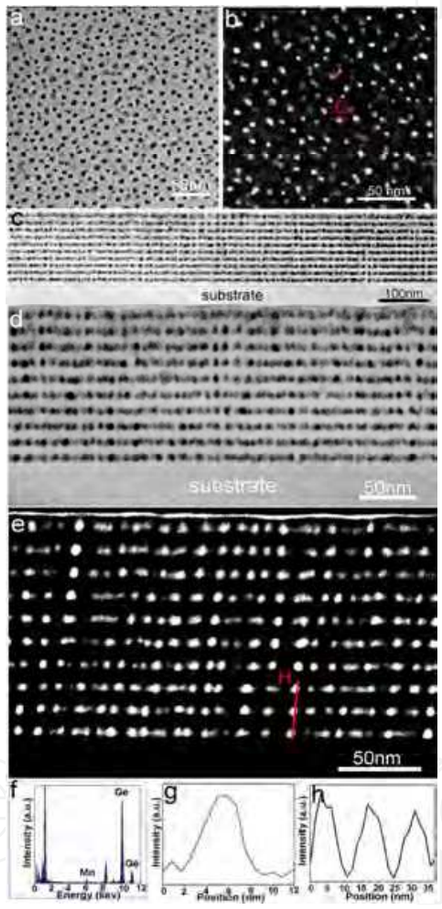

Fig. 5. Transmission electron microscopy (TEM), scanning TEM and energy dispersive X-ray spectroscopy (EDS) results of the multilayer MnGe nanodots. (a), a typical low magnification plane-view TEM image, in which the dark spots are MnGe nanodots. (b), the STEM plane view image. The white spots indicate the MnGe nanodots. (c), a low magnification cross-sectional view. Ordered MnGe nanodots (dark) are clearly seen. (d), a higher magnification TEM image. (e), the STEM cross-section image. The white spots denote the MnGe nanodots. (f), the EDS profile, showing the Mn and Ge peaks. (g, h), line scan profiles of the marked line in (b), (e) using Mn *K* peak, respectively, confirming that the white spots are Mn-rich nanodots.

Based on the magnified cross-sectional image shown in Figure 5d, the nanodot arrays are clearly observed with 10 stacks along the growth direction although not perfectly vertical. In order to determine the composition of the dark dots, EDS analyses in the STEM mode were carried out and typical plane-view and cross-sectional STEM images are shown in Figure 12b and e, respectively. Figure 5f is the EDS result taken from a typical dot and shows clearly the Mn and Ge peaks. Figure 5g and h present EDS line scans using the Mn *K* peak for the dots marked by G and H in Figure 5b and e, respectively, indicating high concentrations of Mn inside the dots. Taking all these comprehensive TEM results into account, it is concluded that the nanodots are Mn-rich when compared with the surrounding matrix.

5.3 Magnetotransport properties of nanodot arrays

The resistivity measurements were carried out to probe the carrier transport under different temperatures. It was found that the temperature-dependent resistivities rapidly increase with decreasing temperature due to the carrier freeze-out effect at low temperatures, which is typically observed in doped semiconductors. (Sze, 1981) Considering the embedded MnGe nanodots, the rise in resistivities at low temperatures also suggests a strong localization of carriers, which takes place at the Mn sites and/or at the MnGe/Ge interfaces, similar to the scenario of MnSb clusters in InMnSb crystals. (Ohno et al., 1999) The temperature dependent resistivity can be generally described by (Ma et al., 2005)

$$\rho(T) = \rho_0 \exp[(\frac{T_0}{T})^{1/\alpha}] \tag{2}$$

where $\rho(T)$ is the temperature-dependent resistivity; ρ_0 and T_0 denote material parameters, a is a dimensionality parameter: $\alpha = 2$ for one-dimensional (1D), $\alpha = 3$ for 2D, and $\alpha = 4$ for 3D systems. In order to reveal the carrier transport mechanisms at different temperature regions, fittings were performed in the plots of lnρ as a function of T^{-a} (Figure 6a). The best fittings were found when a equals to 1 and 4 in the high-temperature and low-temperature regions, respectively, corresponding to the carrier transport via the band conduction (Han et al., 2003) (thermal activation of acceptors) and the 3D Mott's variable range hopping processes. (Ma et al., 2005) According to the fitting results to Equation (2), the obtained nanodot arrays show a dominated hopping process below 10 K. At such a low temperature, the majority of free holes are recaptured by the acceptors. As a result, the free-hole band conduction becomes less important and hole hopping directly between acceptors in the impurity band contributes mostly to the conductivity. (Han et al., 2003) Above 100 K, the conduction is dominated by the thermal activation of the holes (the band conduction). A thermal activation energy (E_a) of 15 meV can be obtained from Equation (2) with $\alpha = 1$ and $E_a = T_0 K_B$, where K_B is the Boltzmann constant. This activation energy does not correspond to any known acceptor energy levels due to Mn doping in Ge, consistent with results shown in Ref. (Pinto et al., 2005a).

To explore practical applications for our extraordinary nanodot arrays, the MR measurements were performed from 2 to 300 K with an external magnetic field up to 10 Tesla. Figure 6b shows the plots of temperature-dependent MR at given magnetic fields (5 and 10 Tesla) for the nanodot arrays. Under a strong magnetic field, the MR in the region of variable range-hopping conduction can be described by (Schlovskii, 1984, Bottger, 1985)

$$MR(H) = \exp[\frac{C}{(\lambda^2 T)^{1/3}}] - 1 \tag{3}$$

where the magnetic length λ equals to $(c\hbar / eH)^{1/2}$ and C is a field and temperature independent constant. Note that the Equation (3) is only valid in a strong-field limit. (Schlovskii, 1984, Ganesan and Bhat, 2008, Bottger, 1985) The inset in Figure 6b shows the best fitting results, in which a linear behavior of MR versus $T^{-1/3}$ is obtained, further confirming the hopping conduction mechanisms ($T \leq 8$ K). Note that the absolute values of MRs were used for the fitting purpose. These fitting results are reasonably close to the obtained hopping regions determined from the zero-magnetic-field resistivity measurements ($T \leq 10$ K, Figure 6a).

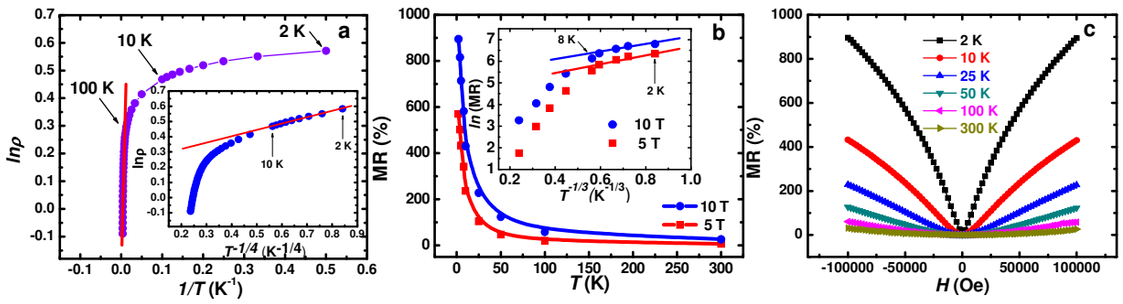

Fig. 6. Magneto-transport measurements for the MnGe nanodot arrays ((A)~(C)) and the nanocolumns ((D)~(F)). For the MnGe nanodot arrays, (A) shows the temperature-dependent resistivity (lnρ vs T^{-1}) and the inset displays the plot of lnρ vs $T^{-1/4}$; (B) is temperature-dependent magneto-resistance (MR) under fixed magnetic fields of 5 and 10 Tesla and inset shows the plot of ln(MR) vs $T^{-1/3}$; (C) demonstrates positive MRs at different temperatures and different magnetic fields.

It is striking to observe that the coherent MnGe nanodot arrays present a large and positive MR up to 900 % at 2 K (Figure 6c). Traditionally, the positive MR is attributed to the Lorentz force in the semiconductor matrix, which deflects the carriers during the transport process. (Ganesan and Bhat, 2008) The resulting MR is positive and proportional to $(\mu H)^2$ under low magnetic fields ($H \leq 1$ Tesla in our case) where μ is the semiconductor mobility (units $m^2V^{-1}S^{-1}$ or T^{-1}) and H is the magnetic field. However, with a simple calculation, the estimated orbital MR is too small to explain the large MR observed from the nanodot arrays. Instead, we anticipate that, besides the effect of orbital MR, the high-density magnetic nanodots could significantly contribute to the large MR ratios due to an enhanced geometric MR effect, from which the current path may be significantly deflected when external magnetic fields were applied to the magnetic nanostructures. (Yuldashev et al., 2001, Solin et al., 2000) To elucidate the underlying physics of the geometrical effect, we consider a thin Hall bar geometry with a measurement current applied in the x-direction, a Hall voltage in the y direction, z direction normal to the sample surface, and an external magnetic field H parallel to z. For semiconductors, the current density and the total electric field can be described by $j = \bar{\sigma} E$, where the magneto-conductivity tensor is given by (Yuldashev et al., 2001, Solin et al., 2000)

$$\bar{\sigma}(H) = \begin{pmatrix} \frac{\sigma}{1+\beta^2} & \frac{\sigma\beta^2}{1+\beta^2} & 0 \\ \frac{-\sigma\beta^2}{1+\beta^2} & \frac{\sigma}{1+\beta^2} & 0 \\ 0 & 0 & \sigma \end{pmatrix}. \quad (4)$$

Here, $\beta = \mu H$. At zero magnetic field, β vanishes. The conductivity tensor is diagonal when lacking of the magnetic field; and the current density can be simply described by $j = \sigma E$. Since the electric field is normal to the surface of a metallic inclusion and *j* ll σ*E*, the current flowing through the material is concentrated into the metallic region which behaves like a "short circuit". As a result, the inclusion of metallic clusters can lead to a higher conduction than that of a homogeneous semiconductor. (Yuldashev et al., 2001, Solin et al., 2000) However, at high magnetic fields ($\beta >> 1$), the off-diagonal terms of $\bar{\sigma}(H)$ dominate. Equivalently, the Hall angle between *j* and *E* approaches 90^o ($j \perp E$); and the current becomes tangent to the nanodots. This further indicates that the current is deflected to flow around the nanodots, resembling an "open circuit" state. The transition from the "short circuit" at the zero field to the "open circuit" at high fields produces an increase of resistance, *i.e.*, a positive geometrically-enhanced MR. (Solin et al., 2000)

5.4 Discussions

The introduction of high percentage Mn (x~20%) generates metallic behavior in Mn doped Ge. Such heavily doped samples possess nanoscale MnGe dots. With a superlattice approach, we have successfully fabricated extraordinarily coherent and self-organized MnGe nanodot arrays embedded in the Ge and GaAs matrixes by low temperature MBE. A high yield of such aligned nanodot arrays was confirmed on different substrates, showing an ideal controllability and reproducibility. More importantly, giant positive magneto-resistances were obtained due to the geometrically-enhanced effect. We anticipate that these studies will advance the development of MnGe magnetic semiconductors and/or other similar systems. The obtained coherent and self-assembled nanostructures could be potentially used as the building blocks in the high-density magnetic memories, sensors, MTJs, and other spintronic devices, enabling a new generation of low dissipation magnetoelectronic devices.

6. Summary and prospectives

This chapter is a review of theoretical and experimental progress that has been achieved in understanding ferromagnetism and related electronic properties in the Mn_xGe_{1-x} DMSs and MnGe metallic nanodots. Interest in DMS ferromagnetism is motivated by the possibility to engineer systems that combine many of the technologically useful features of ferromagnetic and semiconducting materials. This goal has been achieved to an impressive degree in (III, Mn)V DMSs, and further progress can be anticipated in the future. However, due to the low T_c of (III, Mn)V DMSs, the spintronics research seemly reaches a critical bottbleneck, where achieving a high T_c DMS becomes an intriguing and challenging task. Fortunately, the Mn_xGe_{1-x} material system offers a possible route towards higher T_c. The structural and

magnetic properties can be adjusted simply by modifying the system dimensions from 3-D thin films to 0-D quantum dots. A high T_c in excess of 400 K can be obtained and is presumably attributed to the quantum confinement effect, which strengthens the hybridation between the localized Mn impurities and iterant holes. Bound magnetic polarons may also exist since this system falls into a regime where Mn concentrations are much larger than that of holes. Nevertheless, the high T_c in the low-dimentional system suggests that the quantum structure exibit extraordinary properties that significantly differ from these of bulk films. The future progress would rely on the precise theoretical understanding of the quantum confinement effect on ferromagnetism.

It is well known that in order to achieve functioning spintronic devices working at ambient temperatures, it requires the following criteria: (i) the ferromagnetic transition temperature should safely exceed room temperature, (ii) the mobile charge carriers should respond strongly to changes in the ordered magnetic state, and (iii) the material should retain fundamental semiconductor characteristics, including sensitivity to doping and light, and electric fields produced by gate charges. For more than a decade, these three key issues have been the focus of intense experimental and theoretical research. Progress has been also made in achieving field controlled ferromagnetism in (III, Mn)As system, even though the controllability remains at low temperatures because of low T_c. Therefore, the critical challenge now is either to continue increasing T_c in (III, Mn)As, or to look for a new DMS system with both high Curie temperature (Tc>>300 K) and the field controlled ferromagnetism to satisfy all these three criteria. The experimental results of field controlled ferromagnetism in the $Mn_{0.05}Ge_{0.95}$ QDs suggest that the ferromagnetism in this system sensitively responds to the electrical field via the hole mediated effect, similar to that in (III, Mn)As system. Therefore, with a much higher T_c compared with III-V DMS, the Mn_xGe_{1-x} nanostructures could become one of the most promising candidates to achieve room-temperature operation.

On the other hand, the metallic MnGe nanodots with a high percentage of Mn (~20%) show perfect lattice coherence with the Ge matrix. Such a ferrromagnet/semiconudcotr hybrid system is extremely useful owning to their high-quality defect-free interface, where a high efficient spin injection can be realized without a need of oxides such as MgO (spin filter). We also hope to encourage more research efforts in this direction because of the excellent compatibility of MnGe nanodots with the current CMOS technology.

7. References

Ahlers, S., Bougeard, D., Riedl, H., Abstreiter, G., Trampert, A., Kipferl, W., Sperl, M., Bergmaier, A. & Dollinger, G. 2006a. Ferromagnetic Ge(Mn) nanostructures. *Physica E: Low-dimensional Systems and Nanostructures,* 32, 422-425.

Ahlers, S., Bougeard, D., Sircar, N., Abstreiter, G., Trampert, A., Opel, M. & Gross, R. 2006b. Magnetic and structural properties of Ge_xMn_{1-x} films: Precipitation of intermetallic nanomagnets. *Physical Review B (Condensed Matter and Materials Physics),* 74, 214411.

Akai, H. 1998. Ferromagnetism and Its Stability in the Diluted Magnetic Semiconductor (In, Mn)As. *Physical Review Letters,* 81, 3002-3005.

Appelbaum, I. & Monsma, D. J. 2007. Transit-time spin field-effect transistor. *Applied Physics Letters,* 90, 262501.

Arrott, A. 1957. Criterion for Ferromagnetism from Observations of Magnetic Isotherms. *Physical Review,* 108, 1394-1396.

Awschalom, D. D., Loss, D. & Samarth, N. (eds.) 2002. *Semiconductor spintronics and quantum computation*: Springer-Verlag Berlin Heidelberg New York.

Baik, J. M. & Lee, J. L. 2005. Fabrication of vertically well-aligned (Zn,Mn)O nanorods with room temperature ferromagnetism. *Advanced Materials,* 17, 2745-+.

Berciu, M. & Bhatt, R. N. 2001. Effects of Disorder on Ferromagnetism in Diluted Magnetic Semiconductors. *Physical Review Letters,* 87, 107203.

Bhatt, R. N., Berciu, M., Kennett, M. P. & WAN, X. 2002. Diluted Magnetic Semiconductors in the Low Carrier Density Regime. *Journal of Superconductivity,* 15, 71-83.

Biegger, E., Staheli, L., Fonin, M., Rudiger, U. & Dedkov, Y. S. 2007. Intrinsic ferromagnetism versus phase segregation in Mn-doped Ge. *Journal of Applied Physics,* 101, 103912-5.

Bihler, C., Jaeger, C., Vallaitis, T., Gjukic, M., Brandt, M. S., Pippel, E., Woltersdorf, J. & Gosele, U. 2006. Structural and magnetic properties of Mn_5Ge_3 clusters in a dilute magnetic germanium matrix. *Applied Physics Letters,* 88, 112506.

Bolduc, M., Awo-Affouda, C., Stollenwerk, A., Huang, M. B., Ramos, F. G., Agnello, G. & Labella, V. P. 2005. Above room temperature ferromagnetism in Mn-ion implanted Si. *Physical Review B,* 71, 033302.

Bottger, H., Bryksin, V. 1985. *Hopping conduction in solids.,* Berlin, Akademie-Verlag.

Bougeard, D., Ahlers, S., Trampert, A., Sircar, N. & Abstreiter, G. 2006. Clustering in a Precipitate-Free GeMn Magnetic Semiconductor. *Physical Review Letters,* 97, 237202.

Boukari, H., Kossacki, P., Bertolini, M., Ferrand, D., Cibert, J., Tatarenko, S., Wasiela, A., Gaj, J. A. & Dietl, T. 2002. Light and Electric Field Control of Ferromagnetism in Magnetic Quantum Structures. *Physical Review Letters,* 88, 207204.

Brieler, F. J., Grundmann, P., Froba, M., Chen, L. M., Klar, P. J., Heimbrodt, W., Von Nidda, H. A. K., Kurz, T. & Loidl, A. 2004. Formation of Zn1-xMnxS nanowires within mesoporous silica of different pore sizes. *Journal Of The American Chemical Society,* 126, 797-807.

Brunner, K. 2002b. Si/Ge nanostructures. *Reports on Progress in Physics,* 65, 27-72.

Chang, Y. Q., Wang, D. B., Luo, X. H., Xu, X. Y., Chen, X. H., LI, L., Chen, C. P., Wang, R. M., Xu, J. & Yu, D. P. 2003. Synthesis, optical, and magnetic properties of diluted magnetic semiconductor Zn_{1-x} Mn_xO nanowires via vapor phase growth. *Applied Physics Letters,* 83, 4020-4022.

Chen, H., Zhu, W., Kaxiras, E. & Zhang, Z. 2009. Optimization of Mn doping in group-IV-based dilute magnetic semiconductors by electronic codopants. *Physical Review B (Condensed Matter and Materials Physics),* 79, 235202.

Chen, J., Wang, K. L. & Galatsis, K. 2007a. Electrical field control magnetic phase transition in nanostructured Mn_xGe_{1-x}. *Applied Physics Letters,* 90, 012501.

Chen, Y. F., Lee, W. N., Huang, J. H., Chin, T. S., Huang, R. T., Chen, F. R., Kai, J. J., Aravind, K., Lin, I. N. & Ku, H. C. 2005. Growth and magnetic properties of self-assembled (In, Mn)As quantum dots. *Journal of Vacuum Science & Technology B: Microelectronics and Nanometer Structures,* 23, 1376-1378.

Chen, Y. X., Yan, S.-S., Fang, Y., Tian, Y. F., Xiao, S. Q., Liu, G. L., Liu, Y. H. & Mei, L. M. 2007b. Magnetic and transport properties of homogeneous Mn_xGe_{1-x} ferromagnetic semiconductor with high Mn concentration. *Applied Physics Letters,* 90, 052508.

Chiba, D., Matsukura, F. & Ohno, H. 2006a. Electric-field control of ferromagnetism in (Ga,Mn)As. *Applied Physics Letters,* 89, 162505.

Chiba, D., Matsukura, F. & Ohno, H. 2006b. Electrical magnetization reversal in ferromagnetic III-V semiconductors. *Journal of Physics D: Applied Physics,* 39, R215-R225.

Chiba, D., Sawicki, M., Nishitani, Y., Nakatani, Y., Matsukura, F. & Ohno, H. 2008. Magnetization vector manipulation by electric fields. *Nature,* 455, 515-518.

Cho, S., Choi, S., Hong, S. C., Kim, Y., Ketterson, J. B., Kim, B.-J., Kim, Y. C. & Jung, J.-H. 2002. Ferromagnetism in Mn-doped Ge. *Physical Review B,* 66, 033303.

Cho, Y. J., Kim, C. H., Kim, H. S., Lee, W. S., Park, S.-H., Park, J., Bae, S. Y., Kim, B., Lee, H. & Kim, J.-Y. 2008. Ferromagnetic $Ge_{1-x}M_x$ (M = Mn, Fe, and Co) Nanowires. *Chemistry of Materials,* 20, 4694-4702.

Cho, Y. M., Yu, S. S., Ihm, Y. E., Lee, S. W., Kim, D., Kim, H., Sohn, J. M., Kim, B. G., Kang, Y. H., Oh, S., Kim, C. S. & Lee, H. J. 2006. Neutron irradiation effects on polycrystalline Ge1-xMnx thin films grown by MBE. *Current Applied Physics,* 6, 482-485.

Choi, H.-J., Seong, H.-K., Chang, J., Lee, K.-I., Park, Y.-J., Kim, J.-J., Lee, S.-K., He, R., Kuykendall, T. & Yang, P. 2005a. Single-Crystalline Diluted Magnetic Semiconductor GaN:Mn Nanowires. *Advanced Materials,* 17, 1351-1356.

Choi, H. J., Seong, H. K., Chang, J., Lee, K. I., Park, Y. J., Kim, J. J., Lee, S. K., He, R. R., Kuykendall, T. & Yang, P. D. 2005b. Single-crystalline diluted magnetic semiconductor GaN : Mn nanowires. *Advanced Materials,* 17, 1351-+.

Collins, B. A., Chu, Y. S., He, L., Zhong, Y. & Tsui, F. 2008. Dopant stability and strain states in Co and Mn-doped Ge (001) epitaxial films. *Physical Review B (Condensed Matter and Materials Physics),* 77, 193301.

Cui, J. B. & Gibson, U. J. 2005. Electrodeposition and room temperature ferromagnetic anisotropy of Co and Ni-doped ZnO nanowire arrays. *Applied Physics Letters,* 87, 133108.

D'orazio, F., Lucari, F., Passacantando, M., Santucci, P. P. S. & Verna, A. Magneto-optical study of Mn ions implanted in Ge. Magnetics Conference, 2002. INTERMAG Europe 2002. Digest of Technical Papers. 2002 IEEE International, 2002. BB9.

D'orazio, F., Lucari, F., Pinto, N., Morresi, L. & Murri, R. 2004. Toward room temperature ferromagnetism of Ge:Mn systems. *Journal of Magnetism and Magnetic Materials,* 272-276, 2006-2007.

D'orazio, F., Lucari, F., Santucci, S., Picozzi, P., Verna, A., Passacantando, M., Pinto, N., Morresi, L., Gunnella, R. & Murri, R. 2003. Magneto-optical properties of epitaxial MnxGe1-x films. *Journal of Magnetism and Magnetic Materials,* 262, 158-161.

Datta, S. & Das, B. 1990. Electronic analog of the electro-optic modulator. *Applied Physics Letters,* 56, 665-667.

Demidov, E., Danilov, Y., Podol'skiĭ, V., Lesnikov, V., Sapozhnikov, M. & Suchkov, A. 2006. Ferromagnetism in epitaxial germanium and silicon layers supersaturated with managanese and iron impurities. *JETP Letters,* 83, 568-571.

Devillers, T., Jamet, M., Barski, A., Poydenot, V., Bayle-Guillemaud, P., Bellet-Amalric, E., Cherifi, S. & Cibert, J. 2007. Structure and magnetism of self-organized $Ge_{1-x}Mn_x$ nanocolumns on Ge(001). *Physical Review B (Condensed Matter and Materials Physics),* 76, 205306.

Dietl, T. 2006. Self-organized growth controlled by charge states of magnetic impurities. *Nature Materials,* 5, 673-673.

Dietl, T., Awschalom, D.D., Kaminska, M., & Ohno, H. 2008. *Spintronics*, Elsevier

Dietl, T. & Ohno, H. 2006. Engineering magnetism in semiconductors. *Materials Today,* 9, 18-26.

Dietl, T., Ohno, H. & Matsukura, F. 2001. Hole-mediated ferromagnetism in tetrahedrally coordinated semiconductors. *Physical Review B,* 63, 195205.

Dietl, T., Ohno, H., Matsukura, F., Cibert, J. & Ferrand, D. 2000. Zener Model Description of Ferromagnetism in Zinc-Blende Magnetic Semiconductors. *Science,* 287, 1019-1022.

Erwin, S. C. & Petukhov, A. G. 2002. Self-Compensation in Manganese-Doped Ferromagnetic Semiconductors. *Physical Review Letters,* 89, 227201.

Fukushima, T., Sato, K., Katayama-Yoshida, H. & Dederichs, P. H. 2006. Spinodal decomposition under layer by layer growth condition and high curie temperature quasi-one-dimensional nano-structure in dilute magnetic semiconductors. *Japanese Journal of Applied Physics Part 2-Letters & Express Letters,* 45, L416-L418.

Gambardella, P., Brune, H., Dhesi, S. S., Bencok, P., Krishnakumar, S. R., Gardonio, S., Veronese, M., Grazioli, C. & Carbone, C. 2005. Paramagnetic Mn impurities on Ge and GaAs surfaces. *Physical Review B,* 72, 045337.

Gambardella, P., Claude, L., Rusponi, S., Franke, K. J., Brune, H., Raabe, J., Nolting, F., Bencok, P., Hanbicki, A. T., Jonker, B. T., Grazioli, C., Veronese, M. & Carbone, C. 2007. Surface characterization of Mn_xGe_{1-x} and $Cr_yMn_xGe_{1-x-y}$ dilute magnetic semiconductors. *Physical Review B (Condensed Matter and Materials Physics),* 75, 125211.

Ganesan, K. & Bhat, H. L. 2008. Growth, magnetotransport, and magnetic properties of ferromagnetic (In,Mn)Sb crystals. *Journal of Applied Physics,* 103, 6.

Gareev, R. R., Bugoslavsky, Y. V., Schreiber, R., Paul, A., Sperl, M. & Doppe, M. 2006. Carrier-induced ferromagnetism in Ge(Mn,Fe) magnetic semiconductor thin-film structures. *Applied Physics Letters,* 88, 222508.

Garzon, S., Zutic, I. & Webb, R. A. 2005. Temperature-Dependent Asymmetry of the Nonlocal Spin-Injection Resistance: Evidence for Spin Nonconserving Interface Scattering. *Physical Review Letters,* 94, 176601.

Gunnella, R., Morresi, L., Pinto, N., Murri, R., Ottaviano, L., Passacantando, M., D'orazio, F. & Lucari, F. 2005. Magnetization of epitaxial MnGe alloys on Ge(1??) substrates. *Surface Science,* 577, 22-30.

Guoqiang, Z., Tateno, K., Sogawa, T. & Nakano, H. 2008. Vertically aligned GaP/GaAs core-multishell nanowires epitaxially grown on Si substrate. *Applied Physics Express*, 064003 (3 pp.).

Han, J. P., Shen, M. R., Cao, W. W., Senos, A. M. R. & Mantas, P. Q. 2003. Hopping conduction in Mn-doped ZnO. *Applied Physics Letters,* 82, 67-69.

Holub, M., Chakrabarti, S., Fathpour, S., Bhattacharya, P., Lei, Y. & Ghosh, S. 2004. Mn-doped InAs self-organized diluted magnetic quantum-dot layers with Curie temperatures above 300 K. *Applied Physics Letters,* 85, 973-975.

Jaeger, C., Bihler, C., Vallaitis, T., Goennenwein, S. T. B., Opel, M., Gross, R. & Brandt, M. S. 2006. Spin-glass-like behavior of Ge:Mn. *Physical Review B (Condensed Matter and Materials Physics),* 74, 045330.

Jamet, M., Barski, A., Devillers, T., Poydenot, V., Dujardin, R., Bayle-Guillemaud, P., Rothman, J., Bellet-Amalric, E., Marty, A., Cibert, J., Mattana, R. & Tatarenko, S.

2006. High-Curie-temperature ferromagnetism in self-organized $Ge_{1-x}Mn_x$ nanocolumns. *Nat Mater,* 5, 653-659.

Jedema, F. J., Heersche, H. B., Filip, A. T., Baselmans, J. J. A. & Van Wees, B. J. 2002. Electrical detection of spin precession in a metallic mesoscopic spin valve. *Nature,* 416, 713-716.

Jeon, H. C., Chung, K. J., Chung, K. J., Kang, T. W. & Kim, T. W. 2004. Enhancement of the ferromagnetic transition temperature in self-assembled $(Ga_{1-x}Mn_x)As$ quantum wires. *Japanese Journal Of Applied Physics Part 2-Letters & Express Letters,* 43, L963-L965.

Jeon, H. C., Jeong, Y. S., Kang, T. W., Kim, T. W., Chung, K. J., Jhe, W. & Song, S. A. 2002. $(In_{1-x}Mn_x)As$ Diluted Magnetic Semiconductor Quantum Dots with Above Room Temperature Ferromagnetic Transition. *Advanced Materials,* 14, 1725-1728.

Ji, Y., Hoffmann, A., Jiang, J. S. & Bader, S. D. 2004. Spin injection, diffusion, and detection in lateral spin-valves. *Applied Physics Letters,* 85, 6218-6220.

Ji, Y., Hoffmann, A., Jiang, J. S., Pearson, J. E. & Bader, S. D. 2007. Non-local spin injection in lateral spin valves. *Journal of Physics D: Applied Physics,* 5.

Johnson, M. & Silsbee, R. H. 1985. Interfacial charge-spin coupling: Injection and detection of spin magnetization in metals. *Physical Review Letters,* 55, 1790.

Jungwirth, T., Sinova, J., Masek, J., Kucera, J. & Macdonald, A. H. 2006. Theory of ferromagnetic (III,Mn)V semiconductors. *Reviews of Modern Physics,* 78, 809-864.

Kanki, T., Tanaka, H. & Kawai, T. 2006. Electric control of room temperature ferromagnetism in a $Pb(Zr_{0.2}Ti_{0.8})O_3/La_{0.85}Ba_{0.15}MnO_3$ field-effect transistor. *Applied Physics Letters,* 89, 242506.

Kazakova, O., Kulkarni, J. S., Holmes, J. D. & Demokritov, S. O. 2005. Room-temperature ferromagnetism in $Ge_{1-x}Mn_x$ nanowires. *Physical Review B,* 72, 094415.

Kelly, D., Wegrowe, J.-E., Truong, T.-K., Hoffer, X. & Ansermet, J.-P. 2003. Spin-polarized current-induced magnetization reversal in single nanowires. *Physical Review B,* 68, 134425.

Kimura, T. & Otani, Y. 2008. Local domain structure of exchange-coupled NiFe/CoO nanowire probed by nonlocal spin valve measurement. *Journal of Applied Physics,* 103, 083915.

Kioseoglou, G., Hanbicki, A. T., Sullivan, J. M., Van 'T Erve, O. M. J., Li, C. H., Erwin, S. C., Mallory, R., Yasar, M., Petrou, A. & Jonker, B. T. 2004. Electrical spin injection from an n-type ferromagnetic semiconductor into a III-V device heterostructure. *Nature Materials,* 3, 799-803.

Koo, H. C., Kwon, J. H., Eom, J., Chang, J., Han, S. H. & Johnson, M. 2009. Control of Spin Precession in a Spin-Injected Field Effect Transistor. *Science,* 325, 1515-1518.

Kulkarni, J. S., Kazakova, O., Erts, D., Morris, M. A., Shaw, M. T. & Holmes, J. D. 2005. Structural and Magnetic Characterization of Ge0.99Mn0.01 Nanowire Arrays. *Chemistry of Materials,* 17, 3615-3619.

Kuroda, S., Nishizawa, N., Takita, K., Mitome, M., Bando, Y., Osuch, K. & Dietl, T. 2007. Origin and control of high-temperature ferromagnetism in semiconductors. *Nature Materials,* 6, 440-446.

Lauhon, L. J., Gudiksen, M. S., Wang, D. & Lieber, C. M. 2002. Epitaxial core-shell and core-multishell nanowire heterostructures. *Nature,* 420, 57-61.

Li, A. P., Wendelken, J. F., Shen, J., Feldman, L. C., Thompson, J. R. & Weitering, H. H. 2005. Magnetism in Mn_xGe_{1-x} semiconductors mediated by impurity band carriers. *Physical Review B,* 72, 195205.

Li, A. P., Zeng, C., Benthem, K. V., Chisholm, M. F., Shen, J., Rao, S. V. S. N., Dixit, S. K., Feldman, L. C., Petukhov, A. G., Foygel, M. & Weitering, H. H. 2007. Dopant segregation and giant magnetoresistance in manganese-doped germanium. *Physical Review B (Condensed Matter and Materials Physics),* 75, 201201.

Li, H., Wu, Y., Guo, Z., Luo, P. & Wang, S. 2006a. Magnetic and electrical transport properties of $Ge_{1-x}Mn_x$ thin films. *Journal of Applied Physics,* 100, 103908.

Li, H., Wu, Y., Liu, T., Wang, S., Guo, Z. & Osipowicz, T. 2006b. Magnetic and transport properties of Ge:Mn granular system. *Thin Solid Films,* 505, 54-56.

Liao, X. Z., Zou, J., Cockayne, D. J. H., Wan, J., Jiang, Z. M., Jin, G. & Wang, K. L. 2001. Annealing effects on the microstructure of Ge/Si(001) quantum dots. *Applied Physics Letters,* 79, 1258-1260.

Lifeng, L., Nuofu, C., Chenlong, C., Yanli, L., Zhigang, Y. & Fei, Y. 2004. Magnetic properties of Mn-implanted n-type Ge. *Journal of Crystal Growth,* 273, 106-110.

Lin, H.-T., Huang, W.-J., Wang, S.-H., Lin, H.-H. & Chin, T.-S. 2008. Carrier-mediated ferromagnetism in p-Si(100) by sequential ion-implantation of B and Mn. *Journal of Physics: Condensed Matter,* 9, 095004.

Liu, C., Yun, F. & Morko , H. 2005. Ferromagnetism of ZnO and GaN: A Review. *Journal of Materials Science: Materials in Electronics,* 16, 555-597.

Liu, H. & Reinke, P. 2008. Formation of manganese nanostructures on the Si(100)-(2X1) surface. *Surface Science,* 602, 986-992.

Liu, L., Chen, N., Wang, Y., Zhang, X., Yin, Z., Yang, F. & Chai, C. 2006. Growth and properties of magnetron cosputtering grown Mn_xGe_{1-x} on Si (001). *Solid State Communications,* 137, 126-128.

Liu, L., Chen, N., Yin, Z., Yang, F., Zhou, J. & Zhang, F. 2004. Investigation of Mn-implanted n-type Ge. *Journal of Crystal Growth,* 265, 466-470.

Lou, X., Adelmann, C., Crooker, S. A., Garlid, E. S., Zhang, J., Reddy, K. S. M., Flexner, S. D., Palmstrom, C. J. & Crowell, P. A. 2007. Electrical detection of spin transport in lateral ferromagnet-semiconductor devices. *Nat Phys,* 3, 197-202.

Lu, W. & Lieber, C. M. 2006. Semiconductor nanowires. *Journal of Physics D: Applied Physics,* 21.

Luo, X., Zhang, S. B. & Wei, S.-H. 2004. Theory of Mn supersaturation in Si and Ge. *Physical Review B,* 70, 033308.

Lyu, P. & Moon, K. 2003. Ferromagnetism in diluted magnetic semiconductor quantum dot arrays embedded in semiconductors. *The European Physical Journal B - Condensed Matter and Complex Systems,* 36, 593-598.

Ma, Y. J., Zhang, Z., Zhou, F., Lu, L., Jin, A. Z. & Gu, C. Z. 2005. Hopping conduction in single ZnO nanowires. *Nanotechnology,* 16, 746-749.

Maekawa, S. 2004. Spin-dependent transport in magnetic nanostructures. *Journal of Magnetism and Magnetic Materials,* 272-276, E1459-E1463.

Maekawa, S. 2006. *Concepts in Spin Electronics,* Oxford University Press.

Majumdar, S., Das, A. K. & Ray, S. K. 2009a. Magnetic semiconducting diode of p-Ge_{1-x} Mn_x/n-Ge layers on silicon substrate. *Applied Physics Letters,* 94, 122505.

Majumdar, S., Mandal, S., Das, A. K. & Ray, S. K. 2009b. Synthesis and temperature dependent photoluminescence properties of Mn doped Ge nanowires. *Journal of Applied Physics,* 105, 024302.

Matsukura, F., Ohno, H., Shen, A. & Sugawara, Y. 1998. Transport properties and origin of ferromagnetism in (Ga,Mn)As. *Physical Review B,* 57, R2037-R2040.

Miyoshi, T., Matsui, T., Tsuda, H., Mabuchi, H. & Morii, K. 1999. Magnetic and electric properties of Mn_5Ge_3/Ge nanostructured films. 85, 5372-5374.

Morresi, L., Pinto, N., Ficcadenti, M., Murri, R., D'orazio, F. & Lucari, F. 2006. Magnetic and transport polaron percolation in diluted GeMn films. *Materials Science and Engineering: B,* 126, 197-201.

Nazmul, A. M., Kobayashi, S. & Tanaka, S. S. M. 2004. Electrical and Optical Control of Ferromagnetism in III-V Semiconductor Heterostructures at High Temperature (~100 K). *Jpn. J. Appl. Phys.,* 43.

Nepal, N., Luen, M. O., Zavada, J. M., Bedair, S. M., Frajtag, P. & El-Masry, N. A. 2009. Electric field control of room temperature ferromagnetism in III-N dilute magnetic semiconductor films. *Applied Physics Letters,* 94, 132505.

Ogawa, M., Han, X., Zhao, Z., Wang, Y., Wang, K. L. & Zou, J. 2009. Mn distribution behaviors and magnetic properties of GeMn films grown on Si (001) substrates. *Journal of Crystal Growth,* 311, 2147-2150.

Ohno, H., Chiba, D., Matsukura, F., Omiya, T., Abe, E., Dietl, T., Ohno, Y. & Ohtani, K. 2000. Electric-field control of ferromagnetism. *Nature,* 408, 944-946.

Ohno, Y., Young, D. K., Beschoten, B., Matsukura, F., Ohno, H. & Awschalom, D. D. 1999. Electrical spin injection in a ferromagnetic semiconductor heterostructure. *Nature,* 402, 790-792.

Ottaviano, L., Passacantando, M., Verna, A., Parisse, P., Picozzi, S., Impellizzeri, G. & PRIOLO, F. 2007. Microscopic investigation of the structural and electronic properties of ion implanted Mn-Ge alloys. *physica status solidi (a),* 204, 136-144.

Park, E. S., Kim, D. H. & Kim, W. T. 2005. Parameter for glass forming ability of ternary alloy systems. *Applied Physics Letters,* 86, 061907.

Park, Y. D., Hanbicki, A. T., Erwin, S. C., Hellberg, C. S., Sullivan, J. M., Mattson, J. E., Ambrose, T. F., Wilson, A., Spanos, G. & Jonker, B. T. 2002. A Group-IV Ferromagnetic Semiconductor: Mn_xGe_{1-x}. *Science,* 295, 651-654.

Park, Y. D., Wilson, A., Hanbicki, A. T., Mattson, J. E., Ambrose, T., Spanos, G. & Jonker, B. T. 2001. Magnetoresistance of Mn:Ge ferromagnetic nanoclusters in a diluted magnetic semiconductor matrix. *Applied Physics Letters,* 78, 2739-2741.

Passacantando, M., Ottaviano, L., D'orazio, F., Lucari, F., Biase, M. D., Impellizzeri, G. & Priolo, F. 2006. Growth of ferromagnetic nanoparticles in a diluted magnetic semiconductor obtained by Mn^+ implantation on Ge single crystals. *Physical Review B (Condensed Matter and Materials Physics),* 73, 195207.

Passacantando, M., Ottaviano, L., Grossi, V., Verna, A., D'orazio, F., Lucari, F., Impellizzeri, G. & Priolo, F. 2007. Magnetic response of Mn-doped amorphous porous Ge fabricated by ion-implantation. *Nuclear Instruments and Methods in Physics Research Section B: Beam Interactions with Materials and Atoms,* 257, 365-368.

Patibandla, S., Pramanik, S., Bandyopadhyay, S. & Tepper, G. C. 2006. Spin relaxation in a germanium nanowire. *Journal of Applied Physics,* 100, 044303.

Paul, A. & Sanyal, B. 2009. Chemical and magnetic interactions in Mn- and Fe-codoped Ge diluted magnetic semiconductors. *Physical Review B (Condensed Matter and Materials Physics),* 79, 214438.

Peressi, M., Debernardi, A., Picozzi, S., Antoniella, F. & Continenza, A. 2005. Half-metallic Mn-doped Si_xGe_{1-x} alloys: a first principles study. *Computational Materials Science,* 33, 125-131.

Philip, J., Punnoose, A., Kim, B. I., Reddy, K. M., Layne, S., Holmes, J. O., Satpati, B., Leclair, P. R., Santos, T. S. & Moodera, J. S. 2006. Carrier-controlled ferromagnetism in transparent oxide semiconductors. *Nat Mater,* 5, 298-304.

Picozzi, S. & Lezaic, M. 2008. Ab-initio study of exchange constants and electronic structure in diluted magnetic group-IV semiconductors. *New Journal of Physics*, 055017.

Pinto, N., Morresi, L., Ficcadenti, M., Murri, R., D'orazio, F., Lucari, F., Boarino, L. & Amato, G. 2005a. Magnetic and electronic transport percolation in epitaxial $Ge_{1-x}Mn_x$ films. *Physical Review B,* 72, 165203

Pinto, N., Morresi, L., Ficcadenti, M., Murri, R., D.Orazio, F., Lucari, F., Boarino, L. & AMATO, G. 2005b. Magnetic and electronic transport percolation in epitaxial $Ge_{1-x}Mn_x$ films. *Physical Review B,* 72, 165203.

Pinto, N., Morresi, L., Gunnella, R., Murri, R., D'orazio, F., Lucari, F., Santucci, S., PICOZZI, P., Passacantando, M. & Verna, A. 2003. Growth and magnetic properties of MnGe films for spintronic application. *Journal of Materials Science: Materials in Electronics,* 14, 337-340.

Poli, N., Urech, M., Korenivski, V. & Haviland, D. B. Spin-flip scattering at Al surfaces. 2006. AIP, 08H701.

Pramanik, S., Bandyopadhyay, S. & Cahay, M. Spin transport in nanowires. Nanotechnology, 2003. IEEE-NANO 2003. 2003 Third IEEE Conference on, 2003. 87-90 vol.2.

Prinz, G. A. 1998. Magnetoelectronics. *Science,* 282, 1660-1663.

Radovanovic, P. V., Barrelet, C. J., Gradecak, S., Qian, F. & Lieber, C. M. 2005. General synthesis of manganese-doped II-VI and III-V semiconductor nanowires. *Nano Letters,* 5, 1407-1411.

Rheem, Y., Yoo, B.-Y., Beyermann, W. P. & Myung, N. V. 2007. Magneto-transport studies of single ferromagnetic nanowire. *Physica status solidi (a),* 204, 4004-4008.

Schilfgaarde, M. V. & Mryasov, O. N. 2001. Anomalous exchange interactions in III-V dilute magnetic semiconductors. *Physical Review B,* 63, 233205.

Schlovskii, B. I., Efros, A. L. 1984. *Electronics properties of doped semiconductors* Berlin, Spinger-Verlag.

Schlovskii, B. I. & L., E. A. 1984. *Electronics properties of doped semiconductors*, Spinger-Verlag.

Schulthess, T. C. & Butler, W. H. 2001. Electronic structure and magnetic interactions in Mn doped semiconductors. *Jounal of Applied Physics,* 89, 7021-7023.

Seong, H.-K., Kim, U., Jeon, E.-K., Park, T.-E., Oh, H., Lee, T.-H., Kim, J.-J., Choi, H.-J. & Kim, J.-Y. 2009. Magnetic and Electrical Properties of Single-Crystalline Mn-Doped Ge Nanowires. *The Journal of Physical Chemistry C,* 113, 10847-10852.

Slater, J. C. 1964. Atomic Radii In Crystals. *Journal of Chemical Physics,* 41, 3199-&.

Solin, S. A., Thio, T., Hines, D. R. & Heremans, J. J. 2000. Enhanced room-temperature geometric magnetoresistance in inhomogeneous narrow-gap semiconductors. *Science,* 289, 1530-1532.

Solomon, G. S., Trezza, J. A., Marshall, A. F. & Harris, J. S. 1996. Vertically aligned and electronically coupled growth induced InAs islands in GaAs. *Physical Review Letters,* 76, 952-955.

Stroppa, A., Picozzi, S., Continenza, A. & Freeman, A. J. 2003. Electronic structure and ferromagnetism of Mn-doped group-IV semiconductors. *Physical Review B,* 68, 155203.

Sugahara, S., Lee, K. L., Yada, S. & Tanaka, M. 2005. Precipitation of amorphous ferromagnetic semiconductor phase in epitaxially grown Mn-doped Ge thin films. *Japanese Journal of Applied Physics Part 2-Letters & Express Letters,* 44, L1426-L1429.

Sze, S. M. 1981. *Physics of Semiconductor Devices,* New York, Wiley.

Tanaka, M. 2002. Ferromagnet (MnAs)/III-V semiconductor hybrid structures. *Semiconductor Science and Technology,* 17, 327-341.

Tsuchida, R., Asubar, J. T., Jinbo, Y. & Uchitomi, N. 2009. MBE growth and properties of GeMn thin films on (001) GaAs. *Journal of Crystal Growth,* 311, 937-940.

Tsui, F., Collins, B. A., He, L., Mellnik, A., Zhong, Y., Vogt, S. & Chu, Y. S. 2007. Combinatorial synthesis and characterization of a ternary epitaxial film of Co and Mn doped Ge (001). *Applied Surface Science,* 254, 709-713.

Tsui, F., He, L., Ma, L., Tkachuk, A., Chu, Y. S., Nakajima, K. & Chikyow, T. 2003. Novel Germanium-Based Magnetic Semiconductors. *Physical Review Letters,* 91, 177203.

Valenzuela, S. O. & Tinkham, M. 2004. Spin-polarized tunneling in room-temperature mesoscopic spin valves. *Applied Physics Letters,* 85, 5914-5916.

Van Der Meulen, M. I., Petkov, N., Morris, M. A., Kazakova, O., Han, X., Wang, K. L., Jacob, A. P. & Holmes, J. D. 2008. Single Crystalline $Ge_{1-x}Mn_x$ Nanowires as Building Blocks for Nanoelectronics. *Nano Letters,* 9, 50-56.

Verna, A., D'orazio, F., Ottaviano, L., Passacantando, M., Lucari, F., Impellizzeri, G. & Priolo, F. 2007. Magneto-optical investigation of high temperature ion implanted Mn_xGe_{1-x} alloy: evidence for multiple contributions to the magnetic response. *physica status solidi (a),* 204, 145-151.

Verna, A., Ottaviano, L., Passacantando, M., Santucci, S., Picozzi, P., D'orazio, F., Lucari, F., Biase, M. D., Gunnella, R., Berti, M., Gasparotto, A., Impellizzeri, G. & Priolo, F. 2006. Ferromagnetism in ion implanted amorphous and nanocrystalline Mn_xGe_{1-x}. *Physical Review B (Condensed Matter and Materials Physics),* 74, 085204.

Wang, H.-Y. & Qian, M. C. Electronic and magnetic properties of Mn/Ge digital ferromagnetic heterostructures: An ab initio investigation. 2006. Journal of Applied Physics, 99, 08D705.

Wang, K. L., Thomas, S. G. & Tanner, M. O. 1995. SiGe band engineering for MOS, CMOS and quantum effect devices. *Journal of Materials Science: Materials in Electronics,* 6, 311-324.

Wang, Y., Xiu, F., Wang, Y., Zou, J., Beyermann, W., Zhou, Y. & Wang, K. 2011. Coherent magnetic semiconductor nanodot arrays. *Nanoscale Research Letters,* 6, 134.

Wang, Y., Zou, J., Zhao, Z., Han, X., Zhou, X. & Wang, K. L. 2008a. Direct structural evidences of $Mn_{11}Ge_8$ and Mn_5Ge_2 clusters in $Ge_{0.96}Mn_{0.04}$ thin films. *Applied Physics Letters,* 92, 101913.

Wang, Y., Zou, J., Zhao, Z., Han, X., Zhou, X. & Wang, K. L. 2008b. Mn behavior in $Ge_{0.96}Mn_{0.04}$ magnetic thin films grown on Si. *Journal of Applied Physics,* 103, 066104.

Weisheit, M., Fahler, S., Marty, A., Souche, Y., Poinsignon, C. & Givord, D. 2007. Electric Field-Induced Modification of Magnetism in Thin-Film Ferromagnets. *Science,* 315, 349-351.

Xie, Q. H., Madhukar, A., Chen, P. & Kobayashi, N. P. 1995. Vertically Self-Organized INAS Quantum Box Islands on Gaas (100). *Physical Review Letters,* 75, 2542-2545.

Xiu, F., Wang, Y., Kim, J., Hong, A., Tang, J., Jacob, A. P., Zou, J. & Wang, K. L. 2010. Electric-field-controlled ferromagnetism in high-Curie-temperature $Mn_{0.05}Ge_{0.95}$ quantum dots. *Nature Materials,* 9, 337-344.

Yada, S., Sugahara, S. & Tanaka, M. 2008. Magneto-optical and magnetotransport properties of amorphous ferromagnetic semiconductor $Ge_{1-x}Mn_x$ thin films. *Applied Physics Letters,* 93, 193108.

Yagi, M., Noba, K.-I. & Kayanuma, Y. 2001. Self-consistent theory for ferromagnetism induced by photo-excited carriers. *Journal of Luminescence,* 94-95, 523-527.

Yu, S. S., Anh, T. T. L., Ihm, Y. E., Kim, D., Kim, H., Hong, S. K., Oh, S., Kim, C. S., Lee, H. J. & Woo, B. C. 2006. Magneto-transport properties of amorphous $Ge_{1-x}Mn_x$ thin films. *Current Applied Physics,* 6, 545-548.

Yuldashev, S. U., Shon, Y., Kwon, Y. H., Fu, D. J., Kim, D. Y., Kim, H. J., Kang, T. W. & Fan, X. 2001. Enhanced positive magnetoresistance effect in GaAs with nanoscale magnetic clusters. *Journal of Applied Physics,* 90, 3004-3006.

Zeng, C., Yao, Y., Niu, Q. & Weitering, H. H. 2006. Linear Magnetization Dependence of the Intrinsic Anomalous Hall Effect. *Physical Review Letters,* 96, 037204.

Zhao, Y.-J., Shishidou, T. & Freeman, A. J. 2003. Ruderman-Kittel-Kasuya-Yosida–like Ferromagnetism in MnxGe1-x. *Physical Review Letters,* 90, 047204.

Zheng, Y. H., Zhao, J. H., Bi, J. F., Wang, W. Z., JI, Y., Wu, X. G. & Xia, J. B. 2007. Cr-doped InAs self-organized diluted magnetic quantum dots with room-temperature ferromagnetism. *Chinese Physics Letters,* 24, 2118-2121.

Zhu, W., Weitering, H. H., Wang, E. G., Kaxiras, E. & Zhang, Z. 2004. Contrasting Growth Modes of Mn on Ge(100) and Ge(111) Surfaces: Subsurface Segregation versus Intermixing. *Physical Review Letters,* 93, 126102.

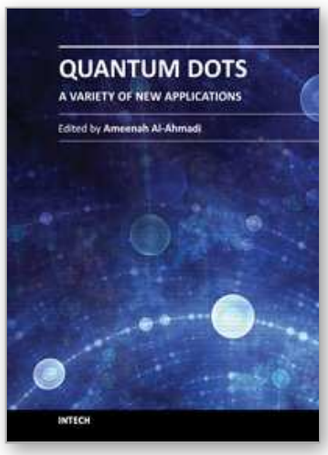

Quantum Dots - A Variety of New Applications

Edited by Dr. Ameenah Al-Ahmadi

ISBN 978-953-51-0483-4
Hard cover, 280 pages
Publisher InTech
Published online 04, April, 2012
Published in print edition April, 2012

The book “Quantum dots: A variety of a new applications” provides some collections of practical applications of quantum dots. This book is divided into four sections. In section 1 a review of the thermo-optical characterization of CdSe/ZnS core-shell nanocrystal solutions was performed. The Thermal Lens (TL) technique was used, and the thermal self-phase Modulation (TSPM) technique was adopted as the simplest alternative method. Section 2 includes five chapters where novel optical and lasing application are discussed. In section 3 four examples of quantum dot system for different applications in electronics are given. Section 4 provides three examples of using quantum dot system for biological applications. This is a collaborative book sharing and providing fundamental research such as the one conducted in Physics, Chemistry, Biology, Material Science, Medicine with a base text that could serve as a reference in research by presenting up-to-date research work on the field of quantum dot systems.

How to reference

In order to correctly reference this scholarly work, feel free to copy and paste the following:

Faxian Xiu, Yong Wang, Jin Zou and Kang L. Wang (2012). Magnetic MnxGe1-x Dots for Spintronics Applications, Quantum Dots - A Variety of New Applications, Dr. Ameenah Al-Ahmadi (Ed.), ISBN: 978-953-51-0483-4, InTech, Available from: http://www.intechopen.com/books/quantum-dots-a-variety-of-new-applications/nanostructured-mnge-dilute-magnetic-quantum-dots-for-spintronics-applications

INTECH
open science | open minds

InTech Europe
University Campus STeP Ri
Slavka Krautzeka 83/A
51000 Rijeka, Croatia
Phone: +385 (51) 770 447
Fax: +385 (51) 686 166
www.intechopen.com

InTech China
Unit 405, Office Block, Hotel Equatorial Shanghai
No.65, Yan An Road (West), Shanghai, 200040, China
中国上海市延安西路65号上海国际贵都大饭店办公楼405单元
Phone: +86-21-62489820
Fax: +86-21-62489821

© 2012 The Author(s). Licensee IntechOpen. This is an open access article distributed under the terms of the Creative Commons Attribution 3.0 License, which permits unrestricted use, distribution, and reproduction in any medium, provided the original work is properly cited.

IntechOpen

IntechOpen